Herzfrequenz und kardiale Repolarisation bei hippokampal generierten Temporallappenanfällen

Inaugural-Dissertation

zur Erlangung des Doktorgrades

der Hohen Medizinischen Fakultät

der Rheinischen Friedrich-Wilhelms-Universität

Bonn

Arthur Jordan

aus Taschkent/Usbekistan

2024

Angefertigt mit der Genehmigung

der Medizinischen Fakultät der Universität Bonn

1. Gutachter: Prof. Dr. Rainer Surges, MHBA
2. Gutachterin: PD Dr. Carmen Pizarro Touron

Tag der Mündlichen Prüfung: 21.06.2024

Aus der Klinik und Poliklinik für Epileptologie

Direktor: Prof. Dr. Rainer Surges, MHBA

Inhaltsverzeichnis

Abkürzungsverzeichnis

Abb.	Abbildung
HF	Herzfrequenz
EEG	Elektroenzephalographie
EKG	Elektrokardiographie
EMG	Elektromyographie
SUDEP	Sudden Unexpected Death in Epilepsy
mTLE	mesiale Temporallappenepilepsie
min	Minute
WI	Wisconsin
TX	Texas
USA	Vereinigte Staaten von Amerika (*United States of America)*
LP	*Limited Partnership*
Hz	Hertz
LAFA	*Low Amplitude Fast Activity*
ASCII	*American Standard Code for Information Interchange*
AUC	*area under the curve*
niAUC	normalisierte iktuale *area under the curve*
S.E.M.	Standardfehler (*Standard Error of the Mean*)
SD	Standardabweichung (*Standard Deviation*)

1. Deutsche Zusammenfassung

1.1 Einleitung

Epileptische Anfälle, insbesondere mit Ursprung im mesialen Temporallappen, können über zentrale autonome Netzwerke Einflüsse auf die Herzaktion ausüben, was sich klinisch häufig als iktuale Zunahme der Herzfrequenz (HF) manifestiert (Garcia et al. 2001; Weil et al. 2005; Moseley et al., 2011; Athira et al. 2023). Auch das seltene, jedoch klinisch unmittelbar relevante Phänomen der iktualen Bradykardie und der Asystolie wurde bevorzugt bei Anfällen temporaler Herkunft beobachtet (Surges et al. 2021). Aber auch passagere Veränderungen der elektrischen Herzeigenschaften, wie beispielsweise der kardialen Repolarisation, erfasst durch Verkürzung oder Verlängerung der HF-korrigierten QT Intervalle, wurden im zeitlichen Zusammenhang mit epileptischen Anfällen beschrieben (Surges et al., 2010). Autonome kardiale und respiratorische Auswirkungen epileptischer Anfälle sind meist gutartig, unter bestimmten Bedingungen und je nach Ausprägung und Dauer können sie jedoch auch beim plötzlichen Tod von Menschen mit Epilepsie (*Sudden Unexpected Death in Epilepsy*, abgekürzt als SUDEP) eine ursächliche Rolle spielen (Thijs et al. 2021; De Lacerda et al. 2023).

Zum sympathischen und parasympathischen autonomen Nervensystem tragen kortikale und subkortikale neuronale Netzwerke im Hirnstamm, der Amygdala, dem Hippokampus und dem insulären Kortex, sowie dem medialen präfrontalen Kortex bei (Cheung et al. 2000; Napadow et al. 2008; Verberne et al. 1998). Erkenntnisse aus Tierversuchen und Untersuchungen am Menschen legen den Schluss einer asymmetrischen Repräsentation der sympathischen und parasympathischen Funktion im Gehirn nahe (Oppenheimer et al. 1992; Zamrini et al. 1990; Koseoglu et al. 2009; Dono et al. 2020). Passend dazu wurden hemisphärenspezifische Auswirkungen transienter pathologischer Zustände des Gehirns, wie beispielsweise epileptischen Anfällen, auf verschiedene Parameter der Herzaktion in der Literatur vielfach beschrieben und von manchen Autoren eine interindividuelle Lateralisation der peri-iktualen HF-Modulation beobachtet (Leutmezer et al., 2003). In anderen Untersuchungen fanden sich keine Lateralisationseffekte über Individuen hinweg (Garcia et al. 2001). In der letztgenannten

Arbeit wurden allerdings nur Patienten untersucht, deren Anfallsursprung auf einer Seite lag. Basierend auf Daten von insgesamt vier Patienten, bei denen sich epileptische Anfälle sowohl rechts- als auch linkshemisphärischen Ursprungs unabhängig voneinander auftraten, wurde in zwei Studien angenommen, dass die peri-iktuale Regulation der HF individuell lateralisiert ist (Kawai et al. 2006; Panchani et al. 2011; Fong et al. 2022). Da die Anfallsursprünge bei den letztgenannten Arbeiten mittels Oberflächen-EEG ermittelt wurden und lediglich 3 Patienten untersucht wurden, ist die Aussagekraft sehr eingeschränkt.

Die bis dato publizierten Arbeiten lassen also keine belastbaren Rückschlüsse darüber zu, ob die als unterschiedlich vermuteten passageren Effekte von Anfällen aus der rechten und linken Hemisphäre auf Herzeigenschaften nicht lediglich auf interindividuellen Unterschieden der untersuchten Patient*Innen beruhen. Der Nachweis einer asymmetrischen Repräsentation der herzmodulierenden Netzwerke wäre von großer klinischer Bedeutung für die Frage, ob die Hemisphärenseite der Anfallsentstehung ein Risikofaktor für anfallsassoziierte kardiale Komplikationen (Asystolien, ventrikuläre Tachyarrhythmien) und SUDEP sind. Die Untersuchung solcher Lateralisationsphänomene ist auch im Zusammenhang mit neuen mobilen Gesundheitstechnologien wichtig, mit deren Hilfe basierend auf anfallsassoziierten HF-Veränderungen epileptische Anfälle automatisiert erkannt werden sollen (Surges 2021).

In der vorliegenden Promotionsarbeit wurde daher ausgehend von der Hypothese, dass autonome kardiale Netzwerke asymmetrisch im Gehirn repräsentiert sind, folgende Fragestellungen untersucht:

(1) Haben im rechten und linken Temporallappen generierte Anfälle unterschiedliche Effekte auf die kardiale Repolsarisation?
(2) Haben im rechten und linken Temporallappen generierte Anfälle unterschiedliche Effekte auf die HF?

Initial untersuchten wir daher an einem Patientenkollektiv mit bilateral implantierten hippokampalen Tiefenelektroden und mehreren unabhängig voneinander auftretenden Anfällen sowohl links- als auch rechtshippokampalen Ursprungs bei jedem Patienten, ob anfallsassoziierte Veränderungen der HF und der kardialen Repolarisation (erfasst als QTc-Intervalle) bei Patienten mit pharmakoresistenter mesialer Temporallappenepilepsie (mTLE) von der Hemisphäre des Anfallsursprungs abhängen. Es dienten dabei Daten aus *manuellen Messungen* der RR-Intervalle, bzw. der HF und der QT-Zeit zu definierten Zeitpunkten als Grundlage (Surges et al. 2013).

Die bei der ersten Arbeit eingesetzte *manuelle Bestimmung* der EKG-Merkmale im epileptischen Anfall ist zwar eine weit verbreitete Methode, basiert aber auf der Analyse ausgewählter Zeitpunkte und bildet daher möglicherweise die peri-iktuale HF-Dynamik nicht adäquat ab (Garcia et al. 2001; Jouven et al., 2005; Nashef et al., 1996; Opherk et al., 2002; Zijlmans et al., 2002). Daher haben wir basierend auf der Hypothese, dass die Betrachtung der HF über den gesamten peri-iktualen Zeitraum zusätzliche Erkenntnisse zur anfallsassoziierten HF-Modulation erbringt, folgende Fragestellung untersucht:

(3) Lassen sich mit einer automatisierten Analyse der peri-iktualen HF neue Merkmale und Lateralisationsphänomene nachweisen?

Dabei sollte an dem hoch selektierten Kollektiv herausgearbeitet werden, ob sich intra- oder interindividuelle Lateralisationseffekte von verschiedenen Merkmalen der HF-Dynamik beobachten lassen. Außerdem sollte geklärt werden, ob markante HF-Veränderungen, wie von einigen Autoren beschrieben, tatsächlich dem elektroenzephalographischen Anfallsursprung vorausgehen können (Hirsch et al., 2015; Kato et al., 2014; Stefanidou et al., 2015).

Die Publikations-Dissertation setzt sich aus einem Artikel im Journal „PLOS ONE“ (Surges et al. 2013), einer Publikation im Journal „Epilepsy Research“ (Jordan et al. 2019) und einem kurzen Artikel (*Letter to the editor*) mit neu generierten Analyseergebnissen im Journal „Clinical Electrophysiology“ (Jordan et al. 2020) zusammen.

1.2 Material und Methoden

1.2.1 Patientenkollektiv

Untersucht wurden die Video-EEG-Daten von insgesamt 205 Patient*Innen mit medikamentös therapierefraktärer Temporallappenepilepsie, die im Zeitraum 2000-2012 eine invasive prächirurgische Evaluation mittels bilateral implantierter Tiefenelektroden in der Klinik für Epileptologie des Universitätsklinikum Bonn durchliefen. Bei der Studie handelt es sich um eine retrospektive Analyse von EEG- und EKG-Daten, die während klinischer Untersuchungen aufgenommen wurden. Einverständniserklärungen von Patienten waren nicht erforderlich, da es sich bei der Studie um eine retrospektive Aufarbeitung handelt und die Patiendaten für die Analyse und die Publikation anonymisiert wurden. Ein positives Votum der hiesigen Ethikkommission zur Analyse solcher Daten liegt vor (laufende Nummer 352/12). Einschlusskriterien für das zu untersuchende Kollektiv war das Vorhandensein von intrakraniellen EEG-Daten und simultanem Einkanal-EKG von mindestens 2 unabhängig voneinander auftretenden, fokal beginnenden Temporallappenanfällen pro Hirnhemisphäre. Eine hinreichende Datenqualität der EEG- sowie EKG-Daten musste zudem gegeben sein. Waren zahlreiche Anfälle für einen Patienten oder eine Seite aufgezeichnet worden, wurden Anfälle ausgesucht, die als stereotyp für den Patienten erachtet wurden, also einander sowohl semiologisch, als auch elektroenzephalographisch am ähnlichsten waren.

Bei 13 Patienten erfolgten die Untersuchungen mittels von posterior eingebrachter hippokampaler Tiefenelektroden (Ad-tech®, Racine, WI, USA, siehe Surges et al. 2013, Abb 1, Tabelle 1), bei einem Patienten erfolgte die Implantation von jeweils 2 Tiefenelektroden pro Hemisphäre in Corpus hippocampi und Amygdala von lateral. Bei einem weiteren Patienten wurden 5 Tiefenelektroden pro Hemisphäre von lateral implantiert, wobei Amygdala, Hippokampus (Caput, Corpus, Cauda) sowie der anteriore entorhinale Kortex und Gyrus parahippocampalis posterior erfasst wurden. Bei allen Patienten wurde die Elektrodenlage im Anschluss an die Implantation durch eine kraniale Kernspintomografie kontrolliert.

1.2.2 Datenerfassung EEG

Die Datenerfassung erfolgte mittels des digitalen Video-EEG-Systems Stellate Harmonie (Version 5.4, Schwarzer GmbH/Natus, Deutschland). Dieses ermöglicht die Verarbeitung von bis zu 128 Kanälen mit einer Abtastrate von 200 Hz bei Analog-Digital-Konversion mit 16 Bit Auflösung. Ein Bandpassfilter für Frequenzbereiche zwischen 0,016 und 70 Hz ist konfigurierbar und zuschaltbar. Die grafische Benutzeroberfläche des Programms erlaubt eine manuelle Befundung sämtlicher Signalkanäle.

Die Bestimmung des Anfallsursprungs, Anfallsbeginns und Anfallsendes, sowie des Zeitpunkts der Ausbreitung der iktualen Aktivität auf die Tiefenelektrode der Gegenseite wurden auf Grundlage des intrakraniellen EEG aus den Tiefenelektroden konventionell manuell ermittelt. Bezüglich des Zeitpunkts des elektrographischen Anfallsbeginns war es in den meisten Fällen möglich, sich an den Markierungen in den Datensätzen und damit am Konsensus der Klinik zu orientieren. Ein typischer Anfall mit Ursprung im Hippokampus beginnt mit einer sog. *low amplitude fast activity* (LAFA) oder hypersynchronen Entladungen (Alarcon et al. 1995, Engel Jr, 2001). Im weiteren Verlauf kommt es bei diesen Anfällen zu einer Abnahme der Signalfrequenz, unter Zunahme der Signalamplitude.

Wichtig für die vorliegende Fragestellung war, dass die iktuale Aktivität auf eine Hemisphäre beschränkt blieb, um einen Einfluss der Gegenseite auf die autonomen Netzwerke und damit auf die Herzaktion weitgehend auszuschließen. Dazu wurde jeder Anfall auf eine „Überleitung“ hin untersucht. Elektroenzephalographisches Merkmal eines übergeleiteten Anfalls ist eine kontinuierliche rhythmische epileptiforme Aktivität in der Tiefenelektrode der Gegenseite.

1.2.3 Manuelle Datenerfassung von EKG-Parametern

Simultan zu EEG und Video wurde bei allen Patienten des Kollektivs auf einem Kanal eine bipolare EKG-Aufzeichnung vorgenommen, die als Grundlage für die Untersuchungen zur Herzaktion im Anfall diente. Dabei handelt es sich um eine modifizierte Einthoven-I-Ableitung mit 2 subklavikulär angebrachten Klebeelektroden.

Die EKG-Aufzeichnung von jedem Anfallsdatensatz wurde sowohl manuell, as auch semi-automatisiert vermessen.

Es erfolgte die manuelle Vermessung von 4 konsekutiven RR-Intervallen und die Bildung des arithmetischen Mittelwertes an jeweils 3 unterschiedlichen Zeitpunkten. Bei jedem Anfall erfolgte eine Messung 1 Minute vor Anfallsbeginn (präiktual), die zweite Messung während des auf eine Hemisphere beschränkten Anfallsaktivität (iktual), sowie eine letzte Messung 1 Minute nach Anfallsende (postiktual), sofern dies der Datensatz zuließ. Bei Anfällen, während derer eine Überleitung auf die Gegenseite stattfand, wurde eine weitere Messung nach der Überleitung gemacht (iktual bilateral). Um die iktuale Messung zu normieren, wurden die iktualen Messungen jeweils am Punkt der größten Abweichung der HF vom präiktualen Wert (meist ist dies der Zeitpunkt mit den kürzesten RR-Intervallen) durchgeführt, da hier der Einfluss der pathologischen Hirnaktivität auf autonome Netzwerke als maximal angenommen wird. Hierbei handelt es sich um eine gängige Herangehensweise bei der Ergometrie und bei kardivaskulären Belastungsstudien (Jouven et al. 2006).

Die QT-Zeiten wurden jeweils vom Beginn des absteigenden Q bis zum Schnittpunkt der Tangente auf der absteigenden T-Welle mit der Isoelektrischen Linie gemessen. Mittels der konsekutiven RR-Intervalle wurde die korrigierte QT-Zeit (QTc) für variable RR-Intervalle errechnet. Hierfür wurden zwecks Fehlerminimierung 4 gängige Formeln herangezogen, da die einzelnen Formeln die QTc-Zeiten über- oder unterschätzen (Aytemir et al. 1999). Folgende Formeln wurden benutzt:

(1) Bazett: $QTc = QT/RR^{1/2}$
(2) Fridericia: $QTc = QT/RR^{1/3}$
(3) Framingham: $QTc = QT + 0{,}154 \times (1-RR)$
(4) Hodges: $QTc = QT + 1{,}75 \times (HF-60)$

In den Formeln (1) - (3) werden QTc-, QT- und RR-Intervalle in Sekunden angegeben. In (4) werden QTc und QT-Intervalle in Millisekunden und die HF in Schlägen pro Minute angegeben.

1.2.4 Halbautomatisierte Untersuchung von EKG-Daten

Um eine Darstellung des HF-Verlaufs über die gesamte Dauer der Anfälle zu bekommen, wurden die Signaldatensätze für jeden Anfall im ASCII-Format aus dem Stellate-Programm exportiert und die EKG-Kanäle mit einem speziell angepassten Algorithmus weiterverarbeitet. Die Implementierung erfolgte im Softwarepaket MATLAB (Version R2011a). Dieser Ansatz hat gegenüber einer manuellen RR-Intervallbestimmung an willkürlich gewählten Zeitpunkten den Vorteil, dass der bei jedem Menschen individuell ausgeprägten HF-Variabilität und respiratorischen Arrhythmie besser Rechnung getragen werden kann und andere Maße der peri-iktualen Herzaktion untersuchbar werden. Für jeden Datensatz erfolgte eine automatische Detektion aller R-Zacken zur Ermittlung von sämtlichen RR-Intervallen und somit zur Erstellung von iktualen Herzfrequenzprofilen über die gesamte Aufzeichnungsdauer. Für die R-Detektion wurde ein Algorithmus von LIBROW^{TM} verwendet (Chernenko 2007), der an die Anforderungen der Studie angepasst und mit einer MATLAB-Implementierung des Pan Tompkins Algorithmus (Sedghamiz 2014) verglichen wurde. Aufgrund des Artefaktreichtums, insbesondere von iktualem EKG, war dennoch eine visuelle Nachbefundung sämtlicher HF-Profile, zwecks Plausibilitätskontrolle notwendig. Es erfolgte zusätzlich eine Extraktion von EMG- und Bewegungsartefakten durch einen auf die vorliegenden Daten abgestimmten Filter, dessen Implementierung ebenfalls in MATLAB erfolgte. Der Filteralgorithmus wurde als MATLAB-Skript mitveröffentlicht (Jordan et al. 2019, Supplementary Section). Algorithmen für eine hinreichend genaue automatisierte Bestimmung der QT-Zeit in artefaktreichen peri-iktualen EKG-Datensätzen standen uns nicht zur Verfügung.

Aus den kontinuierlichen HF-Profilen wurden für jeden Anfall folgende Parameter errechnet:

1. Präiktuale Baseline – der Median aller instantaner HF-Werte der präiktualen Periode (graue horizontale Linie in Abb. 3, Jordan et al. 2019). Diese wurde zum Auffinden falsch positiver HF-Anstiege aufgeteilt in zwei Hälften: die unmittelbare Phase vor dem Anfallsursprung und die nicht-peri-iktuale Phase.
2. Der Median der iktualen HF im Zeitintervall, in dem die Anfallsaktivität auf eine Hemisphäre beschränkt ist (violette horizontle Linie in Abb. 3, Jordan et al. 2019).

3. Der Median der iktualen HF nach Überleitung der Anfallsaktivität auf die kontralaterale Seite
4. Die „normalisierte iktuale area under the curve“ (niAUC), welche ein Maß für die kumulative Wirkung der Anfallsaktivität auf die HF darstellt. Diese wird errechnet, indem von dem Integral der artefaktbereinigten HF-Kurve über der präiktualen Baseline im Zeitraum unilateraler Anfallsaktivität (iktuale AUC, rote Fläche in Abb. 3, , Jordan et al. 2019) die präiktuale AUC subtrahiert wird. Letztere wird errechnet wie die iktuale AUC, hat die gleiche Länge und grenzt unmittelbar an sie an.
5. Die Latenz vom EEG-Anfallsursprung bis zum „HF-Breakpoint“. Letzterer bezeichnet den Beginn des HF-Anstiegs, der anhand eines eigens entwickelten statistischen Algorithmus berechnet wurde. Letzterer wurde ebenfalls als MATLAB-Skript veröffentlicht (Jordan et al. 2019, Supplementary Section).

1.2.5 Statistische Analyse

Statistische Unterschiede von HF und QTc-Werten zwischen Anfällen mit rechts- und linksseitiger Anfallsaktivität aus den *manuell erhobenen* Daten (Surges et al. 2013) wurden paarweise nach dem „mixed linear regression model“ ausgewertet. Dieses korrigierte für variable Anzahlen von Anfällen pro Patient und für individuelle Effekte von Patienten (STATA12 software, StataCorp LP, TX, USA). P-Werte von <0.05 wurden als statistisch signifikant angesehen, basierend auf der Nullhypothese, dass die Seite (Hemisphäre), auf der sich die Anfallsaktivität ausbreitet keinen Einfluss auf die (i) iktale Herzfrequenz und (ii) die QT-Intervalle zu den beschriebenen Zeitpunkten im Anfall nimmt. Alle Daten werden als Mittelwerte ± Standardfehler (S.E.M) angegeben.

Sämtliche statistischen Auswertungen und Datenvisualisierungen für die *halbautomatisiert prozessierten Daten* (Jordan et al. 2019, Jordan et al. wurden mittels MATLAB (R2011a und R2016b) durchgeführt. Die Verteilung der Daten wurde mittels eines Kolmogorow-Smirnow-Anpassungtests geprüft. Für die Hypothesentestung in der Lateralisationsanalyse wurde ein zweiseitiger Wilcoxon-Vorzeichen-Rang-Test herangezogen, wobei p-Werte von <0.05 als statistisch signifikant gewertet wurden. Die Daten wurden als Median ± SD angegeben und als Median ± S.E.M visualisiert.

1.3 Ergebnisse

Fünfzehn (9 Frauen, Alter 35±2,5 Jahre) von insgesamt 205 Patienten mit therapierefraktärer mesialer Temporallappenepilepsie erfüllten die Einschlusskriterien (Surges et al. 2013, Abb. 1). Bei 13 Patienten lagen radiologische Zeichen einer Hippokampussklerose vor, 2 Patienten wiesen keine Auffälligkeiten in der kranialen Kernspintomografie auf. Bei keinem der Patienten des Kernkollektivs lagen vorbeschriebenen kardiopulmonale Erkrankungen vor.

1.3.1 Manuelle HF- und QTc Analyse

Insgesamt wurden 82 Anfälle mit unilateralem hippokampalem Ursprung analysiert (Surges et al. 2013, Tabelle 1). Ein repräsentatives Beispiel einer Darstellung der EEG- und EKG-Spuren eines Anfalls in der grafischen Oberfläche der STELLATE Harmonie Software befindet sich in Abb. 2 (Surges et al. 2013).

Aus den manuellen RR-Intervall Messungen geht ein iktualer HF-Anstieg von ~30% bei auf einen Hippokampus beschränkten Anfällen hervor. Ein signifikanter Unterschied zwischen links- und rechtshippokampalen Anfällen wurde bei den Daten aus den manuellen Messungen nicht gefunden (p=0,411; Surges et al. 2013, Abb. 3A; 4A, B). Im Gegensatz dazu waren die QTc-Intervalle jedoch in signifikant größerem Maße prolongiert während hippokampaler Anfallsaktivität der linken Seite nach Korrektur mit allen 4 Formeln (p-Werte: Bazett 0,016; Fridericia 0,027; Hodges 0,038; Framingham 0,041; Surges et al. 2013, Abb. 3B; 4C, D). Auffallend war, dass zwischen absoluten QTc-Werten und absoluten HF keine Korrellation bestand, sodass keine nennenswerte Verzerrung der Werte durch die Korrekturformeln angenommen werden muss (Surges et al. 2013, Abb. 3C).

Eine deutliche QTc-Prolongation nach Korrektur mit allen 4 Formeln trat in 7 von 41 linkshippokampalen Anfällen bei 4 Patienten und in nur 2 von 37 rechtshippokampalen Anfällen bei 2 Patienten auf (Surges et al. 2013, Tabelle 3). Eine absolute QTc-Verkürzung von unter 10 ms nach allen 4 Korrekturformeln trat in 5 von 37 rechtshippokampalen Anfällen bei 4 Patienten und in 2 linkshippokampalen Anfällen bei 2 Patienten auf. Eine abnormale QTc-Verkürzung wurde nur bei 1 rechtshippokampalen

Anfall gefunden (Surges et al. 2013, Tabelle 3). Es wurden keine potenziell lebensbedrohlichen peri-iktualen kardialen Arrhythmien beobachtet. Lediglich 6 kurze Episoden von Sinusarrhythmie traten ohne konsistenten Zusammenhang zu einer bistimmten Seite des Anfallsursprungs auf.

1.3.2 Halbautomatisierte HF-Analyse

Von den insgesamt für die manuellen Untersuchungen herangezogenen 82 Anfällen mussten 11 für die halbautomatisierten Analysen wegen unzureichender Signalqualität verworfen werden. Vierunddreißig linkshemisphärische und 37 rechtshemisphärische Anfälle hatten eine für weitere Analysen ausreichende Signalqualität. Insgesamt zeigte sich der LIBROW-R-Detektionsalgorithmus robuster bei Vorhandensein von Artefakten im EKG-Signal.

Die kontinuierlichen HF-Profile ergaben eine ausgeprägte Variabilität der HF während und vor hippokampalen Anfällen (Jordan et al. 2019, Abb. 2), wodurch die Vorzüge der halbautomatisierten Analysemethode gegenüber dem manuellen Ansatz deutlich werden. So kam es bei 91 % der linkshippokampalen und 70 % der rechtshippokampalen Anfälle während der unilateralen Phase zu einem HF-Anstieg auf über 100/min, jedoch wird erst durch die kontinuierlichen HF-Profile ersichtlich, dass auch in 21 % der links- und in 28 % der rechtshippokampalen Anfälle ein HF-Anstieg über 100/min bereits in der *präiktualen* Phase (also vor vermutetem Anfallsbeginn) zu verzeichnen war.

In 50% der links- und 54% der rechtshippokampalen Anfälle kam es während der unilateralen Anfallsepisode einem HF-Anstieg oberhalb von 2 Standardabweichungen über der präiktualen Baseline. Bei 8,5% der Anfälle war diese Bedingung auch in der präiktualen Phase erfüllt (Jordan et al. 2019, Zusatzabbildung 3). Die Anzahl von Anfällen mit signifikantem Herzfrequenzanstieg (> 2 SD) war während bewusst erlebter fokaler Anfälle am niedrigsten und während fokal zu bilateral tonisch-klonischer Anfälle am höchsten (Jordan et al. 2019, Zusatzabbildung 2). Ein signifikanter Unterschied zwischen links- und rechtshippokampalen Anfällen war nicht zu verzeichnen (p=0,24).

Bei keinem der untersuchten Anfälle wurde eine iktuale Bradykardie (HF-Abfall auf unter 60/min oder 2 SD der präiktualen Baseline) beobachtet.

Während des Nachtschlafes zeigte sich ein signifikanter Unterschied der präiktualen HF im Vergleich zum Tagintervall (p=0,0017), jedoch kein signifikanter Unterschied der iktualen HF-Anstiege zwischen Anfällen am Tag und in der Nacht (p=0,24, Jordan et al. 2019, Zusatzabbildung 2). Bei 37 Anfällen (21 links- und 16 rechtshippokampalen) kam es zu einer Überleitung zur kontralateralen Hemisphäre. Das mediane Intervall bis zur Überleitung betrug 42 Sekunden (±38s, Wertebereich: 10-213s) und die mediane Herzfrequenz nach Überleitung 125/min (±21/min, Wertebereich: 78-164/min).

Der Vergleich präiktualer und iktualer HF-Verläufe ergab weder in der halbautomatischen noch in der manuellen Methode signifikante interindividuelle Lateralisationseffekte (p=0,95 und p= 0,58, Jordan et al. 2019, Abb. 4A). Auch im Hinblick auf die niAUC und die Latenzen bis zum HF-Breakpoint unterschieden sich links- und rechtshippokampale Anfälle nicht (p=0,92 bzw. p=0,58, Jordan et al. 2019, Abb. 4B und C). Bei 3 Patienten (13% des Gesamtkollektivs) waren zwischen links- und rechtshippokampaler Anfälle Unterschiede der medianen absoluten HF-Änderung von mehr als 10/min zu verzeichnen (Jordan et al. 2020, Abb. 1A).

Der algorithmisch errechnete HF-Breakpoint wies gegenüber dem im EEG ermittelten Anfallsbeginn eine Verzögerung von im Median 16 (± 22) Sekunden auf. Bei 9 Anfällen lag der HF-Breakpoint außerhalb des auf eine Hemisphäre beschränkten Anfallsintervalls, weshalb diese bei den Latenzanalysen nicht weiter berücksichtigt wurden. In 24% der links- und in 11% der rechtshippokampalen Anfälle ging der HF-Breakpoint dem EEG-Anfallsbeginn voraus. Bei 6 Patienten zeigte sich eine individuelle Lateralisation der Latenz bis zum HF-Breakpoint (Jordan et al. 2020, Abb. 1B). Bei 3 der 6 Patienten wurde der HF-Breakpoint bei linkshippokampalen in weniger als 10 s erreicht, während diese Bedingung bei den anderen 3 Patienten der Subgruppe bei rechtshippokampalen Anfällen erfüllt war.
Die manuelle Methode erwies sich als geeignet, den halbautomatisch ermittelten medianen HF-Anstieg abzuschätzen (Jordan et al. 2019, Abb. 5A, r=0,6), während sich

zwischen den manuell ermittelten HF-Veränderungen und der niAUC eine schwächere Korrelation zeigt (Jordan et al. 2019, Abb. 5B, r=0,4).

Bei 6 der 15 Patienten ist die Interpretation der Befunde nur mit Einschränkungen möglich, da lediglich bilateral hippokampale Tiefenelektroden implantiert wurden (Surges et al. 2013, Abb. 1, Tabelle 1). Bei den verbleibenden 7 Patienten standen neben den bilateral implantierten Tiefenelektroden im Hippokampus auch EEG-Daten aus temporobasalen und temporolateralen Streifen- und Gitter-Elektroden zur Verfügung. Dadurch wird eine Korrelation des räumlichen Ausbreitungsgrades der pathologischen EEG-Aktivität mit HF-Veränderungen ermöglicht. Es erfolgte hierzu eine Analyse der EKG-Daten 1 Minute vor Anfallsbeginn, nach unilateralem hippokampalem Anfallsbeginn (zum Zeitpunkt der höchsten HF, jedoch vor Ausbreitung in andere Regionen als den ipsilateralen Hippokampus), nach Ausbreitung in ipsilaterale neokortikale Areale und schließlich nach Ausbreitung die kontralaterale Hemisphäre (Hippokampus oder neokortikale Areale). Es wurde die Beobschtung gemacht, dass das Ausmaß der iktualen HF-Veränderungen vom Ausmaß der räumlichen Ausbreitung der iktualen Aktivität und nicht von der Anfallsdauer beeinflusst wird (Surges et al. 2013, Zusatzabbildung 2). Dies ist konkordant mit vorherigen Untersuchungen (Epstein et al., 1992).

1.4 Diskussion

In den vorliegenden Studien wurden EKG-Veränderungen bei spontan auftretenden epileptischen Temporallappenanfällen untersucht. Die mesiale Temporallappenepilepsie (mTLE) hat eine hohe Inzidenz und den größten Einfluss auf die Herzaktion im Vergleich zu anderen Epilepsieformen (Weil et al. 2005). Ziel der halbautomatisierten Analysen im Rahmen der vorliegenden Arbeiten war die Entwicklung von Algorithmen zur Analyse von peri-iktualen EKG-Daten und die Anwendung derselben zur Klärung der Frage, ob bestimmte Merkmale der peri-iktualen HF-Dynamik Rückschlüsse auf die Lokalisation der Anfallsursprungszone bei Patient*Innen mit mTLE ermöglichen.

1.4.1 Methodische Betrachtungen

Unsere Daten haben gezeigt, dass die präiktuale Periode beachtliche HF-Schwankungen aufweist. Durch die Registrierung kurzer HF-„Schnappschüsse“ zu definierten Zeitpunkten wird diese Dynamik nicht adäquat abgebildet. Da während der iktualen Phase mehrere HF-Maxima auftreten können, kann die Registrierung der maximalen HF-Abweichung vom präiktualen Ausgangswert zu einer Fehleinschätzung des iktualen HF-Verlaufs führen. Ein robustes und konservatives Maß, die durch den Anfall verursachten HF-Änderungen zu quantifizieren, ist der Median aller präiktualer und iktualer RR-Intervalle. Zur besseren Repräsentation der Gesamtauswirkung epileptischer Anfälle auf die HF führten wir den Parameter niAUC ein. Dieser repräsentiert die Anzahl an „Extra-Herzschlägen“, die durch die Anfallsaktivität hervorgerufen wurden und bezieht durch die Integralbildung die Zeitvariable ein. Wie Abb. 5 (Jordan et al. 2019) zu entnehmen ist, weisen die Ergebnisse der vorgestellten manuellen Messmethode eine stärkere Korrelation mit den halbautomatisch errechneten relativen iktualen HF-Veränderungen als mit der niAUC auf, was den Zusatznutzen letzerer unterstreicht.

So erhöht eine ausgeprägte iktuale Tachykardie über Veränderungen der atrioventrikulären Überleitung das Risiko für potenziell gefährliche Herzrhythmusstörungen (Rugg-Gunn et al. 2004, Schernthaner et al. 1999, Schuele et al. 2007). Verschiedene Autoren bedienen sich unterschiedlicher Definitionen der iktualen Tachykardie. Geläufig sind Überschreitungen der 100/min oder 120/min-Schwelle (Hirsch et al. 2015, Britton et al. 2006), eine Zunahme der HF auf über 20% des Ausgangswertes (Hirsch et al. 2015, Stefanidou et al. 2015), Werte oberhalb einer Standardabweichung vom präiktualen Median (Leutmezer et al. 2003) oder auf Werte oberhalb der achtundneunzigsten Perzentile (Moseley et al. 2011).

Die Berechnung der meisten HF-Merkmale erfordert eine Erstellung kontinuierlicher HF-Profile. Die Verwendung zweier unterschiedlicher R-Detektionsalgorithmen kann aufgrund individueller Stärken der Algorithmen die Genauigkeit der resultierenden HF-Profile verbessern. Der Artefaktreichtum in manchen Datensätzen erforderte eine Nachbearbeitung der resultierenden HF-Profile. Hierzu zählt die Identifizierung und Entfernung der durch die R-Detektionsalgorithmen eingeführten Fehler und die Spline-

Interpolation der fehlenden Daten für die Berechnung der Integrale (niAUC). Vorsicht ist bei artefaktreichem EKG oder bei schlechter Performance der R-Detektionsalgorithmen geboten, da größere interpolierte Datenlücken zu einer Verfälschung der Integrale führen kann. Der MATLAB-Code für das genannte Procedere ist im Supplementary Material einsehbar (Jordan et al. 2019, Online-Version).

1.4.2 Die anfallsassoziierte HF-Modulation ist nicht asymmetrisch repräsentiert

In dem untersuchten Patientenkollektiv mit unabhängigen hippokampalen Anfällen von beiden Seiten waren keine signifikanten interindividuellen Einflüsse der Seite des Anfallsursprungs auf die untersuchten HF-Merkmale zu beobachten. Dies deckt sich mit den Erkenntnissen anderer Autoren (Epstein et al. 1992, Rugg-Gunn et al. 2004, Garcia et al. 2001, Moseley et al. 2011, Opherk et al. 2002, Schernthaner et al. 1999). In mehreren vorangegangenen Arbeiten wurde die Latenz zwischen Anfallsursprung und markanten Herzfrequenzveränderungen untersucht, jedoch wiesen die Studien diverse Schwächen auf. So wurde in einigen Arbeiten der Anfallsursprung auf Grundlage von Oberflächen-EEG bestimmt (Di Gennaro et al., 2004, Kato et al. 2014), was eine zusätzliche Latenz zum eigentlichen Anfallsbeginn in tieferen Hirnregionen wie der Hippokampusformation einführen kann. Andere Studien schlossen nur Patienten mit unilateralem Anfallsursprung ein oder basierten auf Patientenkollektiven mit unausgewogenem Verhältnis zwischen Patienten mit links und rechtsseitigem Anfallsursprung (Kato et al. 2014, Hirsch et al., 2015). Diese Schwächen wurden bei der vorgelegten Arbeit durch das gewählte Studiendesign mit ausgewogenem Verhältnis zwischen links- und rechtshippokampalen Anfällen, ausschließlich durch den Einschluss von Patienten mit unabhängig aus beiden Hippokampi auftretenden Anfällen, sowie die Verwendung von bilateralen hippokampalen Tiefenelektroden zur Bestimmung des Anfallszeitpunkts berücksichtigt und kompensiert.

In der dritten Veröffentlichung der Promotionsarbeit wurde gezeigt, dass bei einem Teil der Patienten individuelle Lateralisationseffekte im Hinblick auf das Ausmaß des iktualen HF-Anstiegs und auf die Latenz bis zum HF-Breakpoint bestehen (Jordan et al. 2020, Abb. 1,). Bei keinem der Patienten im Kollektiv waren *beide* Parameter in signifikantem Ausmaß lateralisiert. Der zeitliche Zusammenhang zwischen Anfallsursprung und HF-

Sprung und das Ausmaß peri-iktualer HF-Veränderungen ist laut unseren Ergebnissen also kein geeigneter klinischer Lateralisationsmarker über Individuen hinweg. Angesichts der hoch komplexen Natur der Entstehungs- und Ausbreitungsdynamik epileptischer Anfälle und der individuellen Ausbildung epileptogener Netzwerke erscheinen die Ergebnisse jedoch plausibel.

1.4.3 Die anfallsassoziierte Modulation der kardialen Repolarisation ist asymmetrisch repräsentiert

Die Ergebnisse der manuellen Untersuchung von QTc-Intervallen im epileptischen Anfall legt eine asymmetrische iktuale Repräsentation der kardialen Repolarisation nahe (Surges et al. 2013). Anhaltspunkte für einen asymmetrischen zerebralen Einfluss auf die kardiale Repolarisation ergaben in der Vergangenheit mehrere Studien, in denen bei Tieren und Menschen mit Schädigungen im zentralen Nervensystem QT-Intervalle untersucht wurden (Sander et al. 1995; Colivicchi et al. 2004). Mangels geeigneter Algorithmen konnte in den vorliegenden Arbeiten keine halbautomatisierte Darstellung kontinuierlicher QT-Zeit-Profile vorgenommen werden. Diese könnte interessante neue Aspekte der peri-iktualen kardialen Repolarisationsdynamik zeigen und ist Gegenstand aktuell laufender Projekte.

1.4.4 Schlussfolgerungen

1. Die HF-Modulation ist bei Anfällen aus dem mesialen Temporallappen nicht lateralisiert. Dies ist vorteilhaft für eine HF-basierte automatisierte Anfallsdetektion durch mobile Gesundheitstechnologien, da so die Anfallsursprungszone vor einem geplanten Einsatz solcher Technologien nicht bestimmt werden muss und etwa gleich hohe Effekte (und Sensitivität) erwartet werden können.
2. Unsere Ergebnisse legen nahe, dass die kardiale Repolaristion asymmetrisch bei mesialen Temporallappenanfällen moduliert wird. Linkshippokampal generierte Anfälle waren häufiger mit signifikanten Verlängerungen der QTc-Intervalle assoziiert als möglichen Hinweis auf ein erhöhtes Risiko ventrikulärer Tachyarrhythmien als selten beschriebene Komplikation epileptischer Anfälle. Dies wurde in größeren Patientenkollektiven bislang jedoch nicht untersucht.

3. Unsere Ergebnisse erlauben eine verbesserte Untersuchung der anfallsassoziierten HF-Dynamik durch Anwendung der hier entwickelten Algorithmen und neuen Parameter zur halbautomatisierten Analyse. So ist die achtundneunzigste Perzentile (>2SD) der HF-Änderungen über einen mehrminütigen Ruhewert am besten als Maß für einen anfallsassoziierten HF-Anstieg geeignet. Wenn möglich, sollte auch der niAUC-Parameter bestimmt werden, da er die Gesamtauswirkung der Anfallsaktivität auf die Herzaktion und damit indirekt auf das autonome Nervensystem abbilden soll. Der hier neu entwickelte HF-Breakpoint-Algorithmus erlaubt zudem die genaue Latenzanalyse zwischen Anfallsbeginn und Auswirkungen auf die Herzaktion. Alle neu entwickelten Algorithmen wurden in Form von MATLAB-Codes veröffentlicht.

1.5 Zusammenfassung

In den vorliegenden Studien wurde ein halbautomatischer Analysevorgang für peri-iktuale EKG-basierte Herzfrequenzprofile entwickelt und auf ein hoch selektiertes Patientenkollektiv mit unabhängig in beiden Hippokampi beginnenden epileptischen Anfällen angewandt. Die beschriebenen Herzfrequenzmerkmale und der „Herzfrequenz-Breakpoint-Algorithmus“ könnten für eine herzfrequenzbasierte Anfallsdetektion oder –prädiktion relevant sein. Als Kernaussage der Studie lässt sich festhalten, dass das Ausmaß der Herzfrequenzveränderungen im hippokampalen Anfall oder die zeitliche Beziehung zwischen einem Herzfrequenzsprung und dem Anfallsbeginn nur bei einem geringen Anteil der Patienten mit bilateraler mesialer Temporallappenepilepsie auf die Seite des Anfallsursprungs hinweisen kann und somit als lateralisierender klinischer Hinweis keinen Stellenwert besitzt. Aus den manuellen QT-Zeit-Analysen ergaben sich Hinweise auf eine stärker ausgeprägte QTc-Zeit-Verlängerung bei linkshippokampalen Anfällen als möglichen Hinweis auf ein erhöhtes Risiko anfallsassoziierter ventrikulärer Herzrhythmusstörungen. Die in der Promotionsarbeit entwickelten Algorithmen zur halbautomatisierten Analyse anfallsassoziierter Herzfrequenz-Dynamik sind als MATLAB Codes frei zugänglich.

1.6 Literaturverzeichnis der deutschen Zusammenfassung

Alarcon G, Binnie CD, Elwes RDC, Polkey CE. Power spectrum and intracranial EEG patterns at seizure onset in partial epilepsy. Electroencephalography and clinical neurophysiology 1995; 94: 326-337.

Athira SB, Pal P, Nair PP, Nanda N, Aghoram R. Cardiovascular autonomic function and baroreflex sensitivity in drug-resistant temporal lobe epilepsy. Epilepsy & Behavior 2023; 138: 109013.

Aytemir K, Maarouf N, Gallagher MM, Yap YG, Waktare JE, Malik M. Comparison of formulae for heart rate correction of QT interval in exercise electrocardiograms. Pacing Clin Electrophysiol 1999; 22: 1397–1401.

Britton JW, Ghearing GR, Benarroch EE, Cascino GD. The ictal bradycardia syndrome: localization and lateralization. Epilepsia 2006; 47: 737–744.

Chernenko S 2007. ECG Processing — R-peaks Detection. http://www.librow.com/articles/article-13 (Zugriffsdatum 30.05.2023)

Cheung RT, Hachinski V. The insula and cerebrogenic sudden death. Arch Neurol 2006; 57: 1685–1688.

Colivicchi F, Bassi A, Santini M, Caltagirone C. Cardiac autonomic derangement and arrhythmias in right-sided stroke with insular involvement. Stroke 2004; 35: 2094-2098.

De Lacerda GC, De Souza TF, Tassi EM, Corrêa Filho WB, Da Silva AS. Heart rate variability in Mesial temporal lobe epilepsy and risk for SUDEP. Journal of the Neurological Sciences 2023; 455.

Dono F, Evangelista G, Vollono C, Russo M, Di Stefano V, Bonanni L, Onofrj M, Sensi SL. Interictal heart rate variability analysis reveals lateralization of cardiac autonomic control in temporal lobe epilepsy. Frontiers in neurology 2020;11: 516940.

Engel Jr J. Mesial temporal lobe epilepsy: what have we learned?. The neuroscientist 2001; 7: 340-352.

Epstein MA, Sperling MR, O'connor MJ. Cardiac rhythm during temporal lobe seizures. Neurology 2001; 42: 50-50.

Fong MW, Norris S, Percy J, Hirsch LJ, Herlopian A. Hemisphere-Dependent Ictal Tachycardia Versus Ictal Bradycardia in a Critically Ill Patient. Journal of Clinical Neurophysiology 2022; 39: 15-8.

Garcia M, D'Giano C, Estelles S, Leiguarda, R, Rabinowicz, A. Ictal tachycardia: its discriminating potential between temporal and extratemporal seizure foci. Seizure 2001; 10: 415-419.

Hirsch M, Altenmüller DM, Schulze-Bonhage A. Latencies from intracranial seizure onset to ictal tachycardia: a comparison to surface EEG patterns and other clinical signs. Epilepsia 2015; 56: 1639-1647.

Jordan A, Bausch M, Surges R. Semi-automatic quantification of seizure-related effects on heart activity. Epilepsy research 2019; 157: 106187.

Jordan A, Bausch M, Surges R. Modulation of ictal heart rate is individually lateralized in temporal lobe epilepsy. Clinical Neurophysiology 2020; 131: 2932-2933.

Jouven X, Empana JP, Schwartz PJ, Desnos M, Ducimetière DCP. Heart-Rate Profile during Exercise as a Predictor of Sudden Death. N Engl J Med 2005; 352: 1951-1958.

Kato K, Jin K, Itabashi H, Iwasaki M, Kakisaka Y, Aoki M, Nakasato N. Earlier tachycardia onset in right than left mesial temporal lobe seizures. Neurology 2014; 83: 1332-1336.

Koseoglu E, Kucuk S, Arman F, Ersoy AO. Factors that affect interictal cardiovascular autonomic dysfunction in temporal lobe epilepsy: role of hippocampal sclerosis. Epilepsy & Behavior 2009; 16: 617-621.

Kawai M, Goldsmith IL, Verma A. Differential effects of left and right hemispheric seizure onset on heart rate. Neurology 2006; 66: 1279–1280.

Leutmezer F, Schernthaner C, Lurger S, Pötzelberger K, Baumgartner C. Electrocardiographic changes at the onset of epileptic seizures. Epilepsia 2003; 44: 348–354.

Moseley BD, Wirrell EC, Nickels K, Johnson JN, Ackerman MJ. Electrocardiographic and oximetric changes during partial complex and generalized seizures. Epilepsy Res 2011; 95: 237–245.

Napadow V, Dhond R, Conti G, Makris N, Brown EN. Brain correlates of autonomic modulation: combining heart rate variability with fMRI. Neuroimage 2008; 42: 169–177.

Nashef L, Walker F, Allen P, Sander JW, Shorvon SD, Fish DR. Apnoea and bradycardia during epileptic seizures: relation to sudden death in epilepsy. Journal of Neurology, Neurosurgery & Psychiatry 1996; 60: 297-300.

Opherk C, Coromilas J, Hirsch LJ. Heart rate and EKG changes in 102 seizures: analysis of influencing factors. Epilepsy Res 2002; 52: 117–127.

Oppenheimer SM, Gelb A, Girvin JP, Hachinski VC. Cardiovascular effects of human insular cortex stimulation. Neurology 1992; 42: 1727–1732.

Page T, Rugg-Gunn FJ. Bitemporal seizure spread and its effect on autonomic dysfunction. Epilepsy & Behavior 2018; 84: 166-172.

Panchani J, Adjei P, Henneberger C, Scott CA, Thompson AJ.
Asymmetric hemispheric representation of periictal heart rate modulation is individually lateralised. Epileptic Disord 2011; 13: 172–176.

Rugg-Gunn FJ, Simister RJ, Squirrell M, Holdright DR, Duncan JS. Cardiac arrhythmias in focal epilepsy: a prospective long-term study. The Lancet 2004; 364: 2212-2219.

Sander D, Klingelhöfer J. Changes of circadian blood pressure patterns and cardiovascular parameters indicate lateralization of sympathetic activation following hemispheric brain infarction. Journal of neurology 1995; 242: 313-318.

Schernthaner C, Lindinger G, Pötzelberger K, Zeiler K, Baumgartner C. Autonomic epilepsy - the influence of epileptic discharges on heart rate and rhythm. Wiener Klinische Wochenschrift 1999; 111: 392-401.

Schuele SU, Bermeo AC, Alexopoulos AV, Locatelli ER, Burgess RC, Dinner DS, Foldvary-Schaefer N. Video-electrographic and clinical features in patients with ictal asystole. Neurology 2007; 69: 434-441.

Sedghamiz H 2014. Complete Pan Tompkins Implementation ECG QRS Detector - File Exchange - MATLAB Central. https://de.mathworks.com/matlabcentral/fileexchange/45840-complete-pan-tompkins-implementation-ecg-qrs-detector (Zugriffsdatum 30.05.2023)

Stefanidou M, Carlson C, Friedman D. The relationship between seizure onset zone and ictal tachycardia: An intracranial EEG study. Clinical neurophysiology 2015; 126: 2255-2260.

Surges R. Wearables bei Epilepsien. Klin Neurophysiol 2021; 52: 29–38.

Surges R, Scott CA, Walker MC. Enhanced QT shortening and persistent tachycardia after generalized seizures. Neurology 2010; 74: 421-6.

Surges R, Jordan A, Elger CE. Ictal modulation of cardiac repolarization, but not of heart rate, is lateralized in mesial temporal lobe epilepsy. PloS one 2013; 8: e64765.

Surges R, Shmuely S, Dietze C, Ryvlin P, Thijs RD. Identifying patients with epilepsy at high risk of cardiac death: signs, risk factors and initial management of high risk of cardiac death. Epileptic Disord. 2021; 23: 17-39.

Thijs RD, Ryvlin P, Surges R. Autonomic manifestations of epilepsy: emerging pathways to sudden death?. Nat Rev Neurol. 2021; 17: 774-788.

Verberne AJ, Owens NC. Cortical Modulation of the Cardiovascular System. Progress in neurobiology 1998; 54: 149-168.

Weil S, Arnold S, Eisensehr I, Noachtar S. Heart rate increase in otherwise subclinical seizures is different in temporal versus extratemporal seizure onset: support for temporal lobe autonomic influence. Epileptic Disorders. 2005; 7: 199-204.

Zamrini EY, Meador KJ, Loring DW, Nichols FT, Lee GP. Unilateral cerebral inactivation produces differential left/right heart rate responses. Neurology 1990; 40: 1408–1411.

Zijlmans M, Flanagan D, Gotman J. Heart rate changes and ECG abnormalities during epileptic seizures: prevalence and definition of an objective clinical sign. Epilepsia 2002; 43: 847-854.

2. Veröffentlichungen

OPEN ACCESS Freely available online

PLOS ONE

Ictal Modulation of Cardiac Repolarization, but Not of Heart Rate, Is Lateralized in Mesial Temporal Lobe Epilepsy

Rainer Surges*, Arthur Jordan, Christian E. Elger

Department of Epileptology, University Hospital Bonn, Bonn, Germany

Abstract

Objectives: Human and animal studies provided controversial data on asymmetric cortical representation of cardiac function, which may partially be due to different study designs and inter-individual variability. Here, we investigated whether seizure-related changes in heart rate (HR) and cardiac repolarization depend on the side of seizure-activity in people with mesial temporal lobe epilepsy (mTLE).

Methods: To account for inter-individual variability, EEG and ECG data were reviewed from patients with medically refractory mTLE undergoing pre-surgical video-EEG telemetry with at least 2 seizures arising from each hippocampus as assessed by bilateral hippocampal depths electrodes. RR and QT intervals were determined at different timepoints using a one-lead ECG. QT intervals were corrected for HR (QTc) using 4 established formulas.

Results: Eighty-two seizures of 15 patients were analyzed. HR increased by ~30% during hippocampal activity irrespective of the side ($p = 0.411$). QTc intervals were lengthened to a significantly greater extent during left hippocampal seizures (e.g. difference of QT intervals between preictal and ictal state using Bazett's formula; left side 32.0 ± 5.3 ms, right side 15.6 ± 7.7 ms; $p = 0.016$). Abnormal QTc prolongation occurred in 7 of 41 left hippocampal seizures of 4 patients, and only in 2 of 37 right hippocampal seizures of 2 patients.

Conclusions: Seizure-related modulation of cardiac repolarization, but not of HR, appears to depend on the side of ictal activity, strengthening the hypothesis of asymmetric cerebral representation of cardiac function. The clinical relevance of this is unclear, but may indicate an increased risk of abnormal ictal QT prolongation in people with left mTLE.

Citation: Surges R, Jordan A, Elger CE (2013) Ictal Modulation of Cardiac Repolarization, but Not of Heart Rate, Is Lateralized in Mesial Temporal Lobe Epilepsy. PLoS ONE 8(5): e64765. doi:10.1371/journal.pone.0064765

Editor: Mathias Baumert, University of Adelaide, Australia

Received December 28, 2012; **Accepted** April 17, 2013; **Published** May 31, 2013

Funding: Dr. R. Surges has received support for congress participation and speaker fees from EISAI; had a consultancy agreement with UCB; is part of PRISM – the Prevention and Risk Identification of SUDEP Mortality Consortium which is funded by the National Institutes of Health (NBIH/NINDS - 1P20NS076965-01). A. Jordan has no financial disclosure to make. Prof. Dr. C. E. Elger is consultant for Desitin and Novartis and received honoraria for talks from Pfizer and Esai. The funders had no role in study design, data collection and analysis, decision to publish, or preparation of the manuscript.

Competing Interests: The authors have declared that no competing interests exist.

* E-mail: rainer.surges@gmail.com

Introduction

Cardiac activity is dynamically modulated by the autonomic nervous system to ascertain sufficient blood and oxygen supply to all organs in response to various physiologic and pathophysiologic conditions. The major players consist of the sympathetic and parasympathetic branches which are regulated through cortical and subcortical neuronal networks including brain stem, insular cortex, amygdala, and hippocampus [1,2]. Previous studies in human and animals have suggested an asymmetric representation of sympathetic and parasympathetic functions in the brain. For instance, electrical stimulation of the left insula or pharmacological inactivation of the right hemisphere predominantly led to a decrease in heart rate (HR), whereas right-sided stimulation or left-sided inactivation increased HR [3,4]. Disturbances of cardiac repolarization have also been reported with seizures and other neurological conditions such as ischemic stroke [5–11]. Importantly, insults of the right hemisphere with insular involvement appear to be more frequently associated with prolongation of QT interval and potentially serious cardiac arrhythmias, supporting the notion of an asymmetrically represented cortical control of cardiac repolarization [5–7].

Taken together, cardiac function appears to be asymmetrically represented in the brain with potential clinical relevance according to the side of cerebral affection. To date, however, it is unclear whether transient disturbances of brain function e.g. by epileptic seizures have also a hemispheric-specific effect on cardiac function. Previous studies have produced controversial results, maybe due to variable interindividual patterns of cardiac regulation [11–13]. Based on the findings of three cases with seizures independently arising from both hemispheres in a given patient, we have recently hypothesized that periictal regulation of HR is individually lateralized [14,15]. This hypothesis, however, was derived from three patients with scalp EEG recordings only, considerably limiting the strengths of these observations.

Here, we have asked whether seizure-related changes in HR and cardiac repolarization depend on the side of seizure-activity in people with medically refractory mesial temporal lobe epilepsy (mTLE) undergoing pre-surgical video-EEG telemetry using intracranial electrodes. We included patients with bilateral hippocampal depths electrodes and, to account for intrinsic differences in autonomic function and to allow intraindividual comparison, only those who had at least two seizures arising from each hippocampus independently from each other during video-EEG telemetry.

Materials and Methods

Patients and Inclusion Criteria

We reviewed patients with medically refractory mTLE undergoing presurgical video-EEG monitoring during a 12 years period from January 2000 to December 2011 in the Department of Epileptology at the University Hospital Bonn (Germany). This study is a retrospective audit of EEG and ECG data which have been collected during standard clinical procedures, and has been approved as such by the local medical ethics committee ("Ethikkommission an der Medizinischen Fakultaet der Rheinischen Friedrich-Wilhelms-Universitaet Bonn"). Informed patient consent was not required because of the retrospective design and the anonymization of patient-related data for analysis and publication. Inclusion criteria were presence of bilateral hippocampal depth electrodes and the occurrence of at least two seizures with independent onset from each hippocampus. Two to 4 seizures per hemisphere per patient were analyzed. Seizures were selected according to the side of seizure-onset and the interpretability of simultaneous ECG traces. If more than 2–4 seizures per patient and hemisphere were eligible for analysis, seizures were selected in chronological order of occurrence. The correct position of the electrodes was controlled with the help of MRI after implantation. In 13 patients, hippocampal depths electrodes (Adtech®, Racine, WI, USA) were implanted via a posterior approach as displayed in figure 1A and described in table 1. In one patient, the amygdala and the body of the hippocampus were covered by two depths electrodes implanted via a lateral approach, and in the remaining patient, 5 depths electrodes via a lateral approach were implanted on each hemisphere and covered the amygdala, hippocampus (head, body and tail) as well as anterior entorhinal cortex and posterior parahippocampal gyrus.

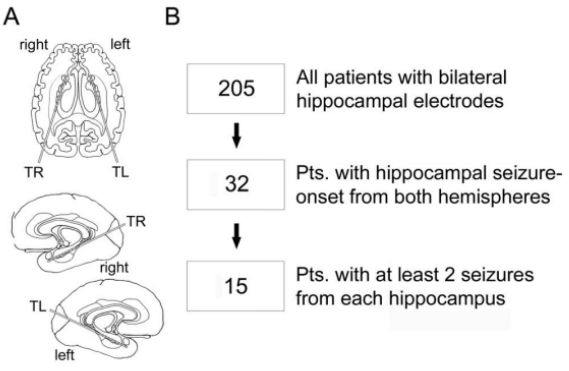

Figure 1. Implantation scheme and flowchart of patient selection. (A) Scheme of implantation of intracranial electrodes to assess hippocampal activity and (B) flowchart of selection and inclusion of patients.
doi:10.1371/journal.pone.0064765.g001

Presurgical Evaluation

Standard presurgical assessment included cerebral MRI (1.5 or 3 Tesla), non-invasive video-EEG telemetry using scalp EEG (10–20 system with additional temporal electrodes) prior to invasive video-EEG telemetry and neuropsychological testing. Video-EEG telemetry is the simultaneous acquisition of a video film (to observe the clinical symptoms of the patients) and EEG recordings (to assess the regional onset and propagation of the seizure activity) in order to correlate the patients' behaviour with the seizure activity. In all included patients, invasive video-EEG monitoring was performed with hippocampal depth electrodes (see above) and in some patients with additional neocortical subdural strip or grid electrodes (table 1). All electrodes were placed in dependence of MRI findings, prior findings in scalp EEG recordings and seizure semiology.

EEG Recordings

EEG data acquisition was performed with a Stellate Harmonie digital video-EEG system (Version 5.4, Schwarzer GmbH/Natus, Germany) using up to 128 channels, a 200 Hz sampling rate and a 16 bit analogue-to-digital converter. Data were band pass filtered between 0.016 and 70 Hz. We determined the timepoint and localization of seizure-onset according to the intracranial EEG recordings.

Periictal One-lead ECG Recordings

A modified lead-I ECG (adhesive electrodes placed below the clavicles of either side) was recorded simultaneously with EEG. RR intervals were determined manually at different timepoints (1 min before EEG seizure-onset, during unilateral hippocampal activity where RR was shortest in order to "normalize" the data; 1 min after seizure cessation). QT intervals were manually measured from the start of the QRS complex to the end of the T wave (defined by the intersection with the isoelectric line). QT and preceding RR intervals were determined from 3–5 successive ECG complexes and QT intervals were corrected for variable RR intervals. All correction formulas tend to over- or underestimate QTc [16]. To minimize errors due to correction bias and as a sensitivity analysis, we have used four established formulas as follows:

(1) Bazett: $QTc = QT/RR^{1/2}$
(2) Fridericia: $QTc = QT/RR^{1/3}$
(3) Framingham: $QTc = QT + 0.154 \times (1\text{-}RR)$
(4) Hodges: $QTc = QT + 1.75 \times (HR - 60)$

In formulas (1)–(3), QTc, QT and RR interval values are expressed in seconds. In (4), QTc and QT intervals are in milliseconds and HR is in beats per minute. To reduce a bias error of putatively pathologic QTc intervals (due to higher HR), we have used modified normal limits for QTc intervals as proposed by Luo and colleagues (see table S1) [17].

Statistics

Statistical differences of HR and QTc values between seizures with left- and right-sided ictal activity were assessed pairwisely using a mixed linear regression model adjusted for variable seizure numbers per patient and individual patient effects (STATA12 software, StataCorp LP, TX, U.S.A.). P-values <0.05 were regarded as statistically significant, based on the null hypothesis that there is no hemispheric side effect on (i) ictal HR and (ii) QT intervals. All data are given as means ± S.E.M.

Table 1. Clinical characteristics of patients.

Patient no.	Sex	Age*/Epilepsy duration*/ handedness	MRI finding	Surgery	Intracranial electrodes	FU[§]/ Outcome[#]
48	M	32/32/R	Bilat. HS	No	Hipp: 1 depth electrode (10 c.) on each side from posterior ExHipp: None	n.a.
105	M	39/3/R	Bilat. HS R>L	No	Hipp: 1 depth electrode (10 c.) on each side from posterior ExHipp: None	n.a.
111	M	28/23/L	HS L	SAHE L	Hipp: 1 depth electrode (10 c.) on each side from posterior ExHipp: 1 temporo-lateral (16 c.) and 2 temporo-basal (4 c.) strip electrodes on left side	48/I
112	F	24/4/R	Bilat. HS L>R	No	Hipp: 1 depth electrode (10 c.) on each side from posterior ExHipp: 1 temporo-lateral (4 c.) and 2 temporo-basal (4 c.) strip electrodes on each side	n.a.
119	F	55/33/R	Bilat. HS L>R	SAHE R	Hipp: 1 depth electrode (10 c.) on each side from posterior ExHipp: 1 temporo-lateral (6 c.) and 2 temporo-basal (4 c.) strip electrodes on each side	53/II
127	M	45/39/L	None	No	Hipp: 1 depth electrode (10 c.) on each side from posterior ExHipp: 1 temporo-lateral (4 c.) and 2 temporo-basal (4 c.) strip electrodes on each side	n.a.
132	F	47/7/R	Bilat. HS	No	Hipp: 1 depth electrode (10 c.) on each side from posterior ExHipp: None	n.a.
135	F	46/33/R	HS R	SAHE R	Hipp: 1 depth electrode (10 c.) on each side from posterior ExHipp: 1 temporo-lateral (6 c.) and 2 temporo-basal (4 c.) strip electrodes on each side	18/II
143	M	22/15/L	None	SAHE L	Hipp: 1 depth electrode (10 c.) on each side from posterior ExHipp: 2 temporo-basal (4 c.) strip electrodes on each side 1 temporo-lateral strip electrode (6 c.) on right side and 1 grid electrode (32 c.) on left side covering Wernicke's area	24/I
144	F	35/30/R	Bilat. HS L>R	No	Hipp: 1 depth electrode (10 c.) on each side from posterior ExHipp: None	n.a.
160	F	31/30/R	Bilat. HS	TL-resection incl. AHE L	Hipp: 1 depth electrode (10 c.) on each side from posterior ExHipp: None	No FU-visit
182	F	34/14/R	Bilat. HS L>R	No	Hipp: 1 depth electrode (10 c.) on each side from posterior ExHipp: None	n.a.
184	F	28/25/L	HS R	No	Hipp: 2 depth electrodes (8 c.) on each side from lateral ExHipp: 2 temporo-basal (4 c.) strip electrodes on each side	n.a.
187	F	31/29/R	Bilat. HS	No	Hipp: 1 depth electrode (10 c.) on each side from posterior ExHipp: 1 temporo-lateral (6 c.) and 2 temporo-basal (4 c.) strip electrodes on each side	n.a.
202	M	28/15/R	HS L	No	Hipp: 5 depths electrodes (10 c.) on each side from lateral ExHipp: 2 frontal strip electrodes (8 c.) on each side	n.a.

*At telemetry.
[§]follow-up in months.
[#]according to Engel classification.
c, electrode contacts; ExHipp, extrahippocampal; Hipp, hippocampal; HS, hipppocampal sclerosis; L, left; n.a., not applicable; R, right; SAHE, selective amygdala-hippocampectomie; TL, temporal lobe.
doi:10.1371/journal.pone.0064765.t001

Results

Fifteen (9 women; age 35.0±2.5 years) of 205 patients with medically refractory mTLE fulfilled the inclusion criteria (Figure 1B). Thirteen patients had signs of hippocampal sclerosis on cerebral MRI and 2 patients had no detectable MRI abnormalities (Table 1). None of the patients had been diagnosed with a cardio-pulmonary disease.

A total of 82 seizures with unilateral hippocampal onset were analyzed (Table 2). A representative example of original EEG- and ECG tracings is given in figure 2. Overall, HR increased by ~30% during seizure activity confined to the hippocampus without significant differences between left- and right-sided seizures ($p = 0.411$; Figure 3A; 4A,B).

QTc intervals, however, were prolonged to a significantly greater extent with ongoing hippocampal seizures on the left side after adjustment with all 4 correction formulas (p-values: Bazett 0.016; Fridericia 0.027; Hodges 0.038; Framingham 0.041; Figure 3B; 4C,D). Importantly, absolute QTc values were not correlated with the absolute HR, suggesting that there was no major bias introduced by using correction formulas (Figure 3C). Abnormal QTc prolongation according to all 4 correction formulas occurred in 7 of 41 left hippocampal seizures of 4 patients, and only in 2 of 37 right hippocampal seizures of 2 patients (Table 3). Absolute QTc shortening below 10 ms according to all 4 correction formulas occurred in 5 of 37 right hippocampal seizures of 4 patients, and in 2 left hippocampal

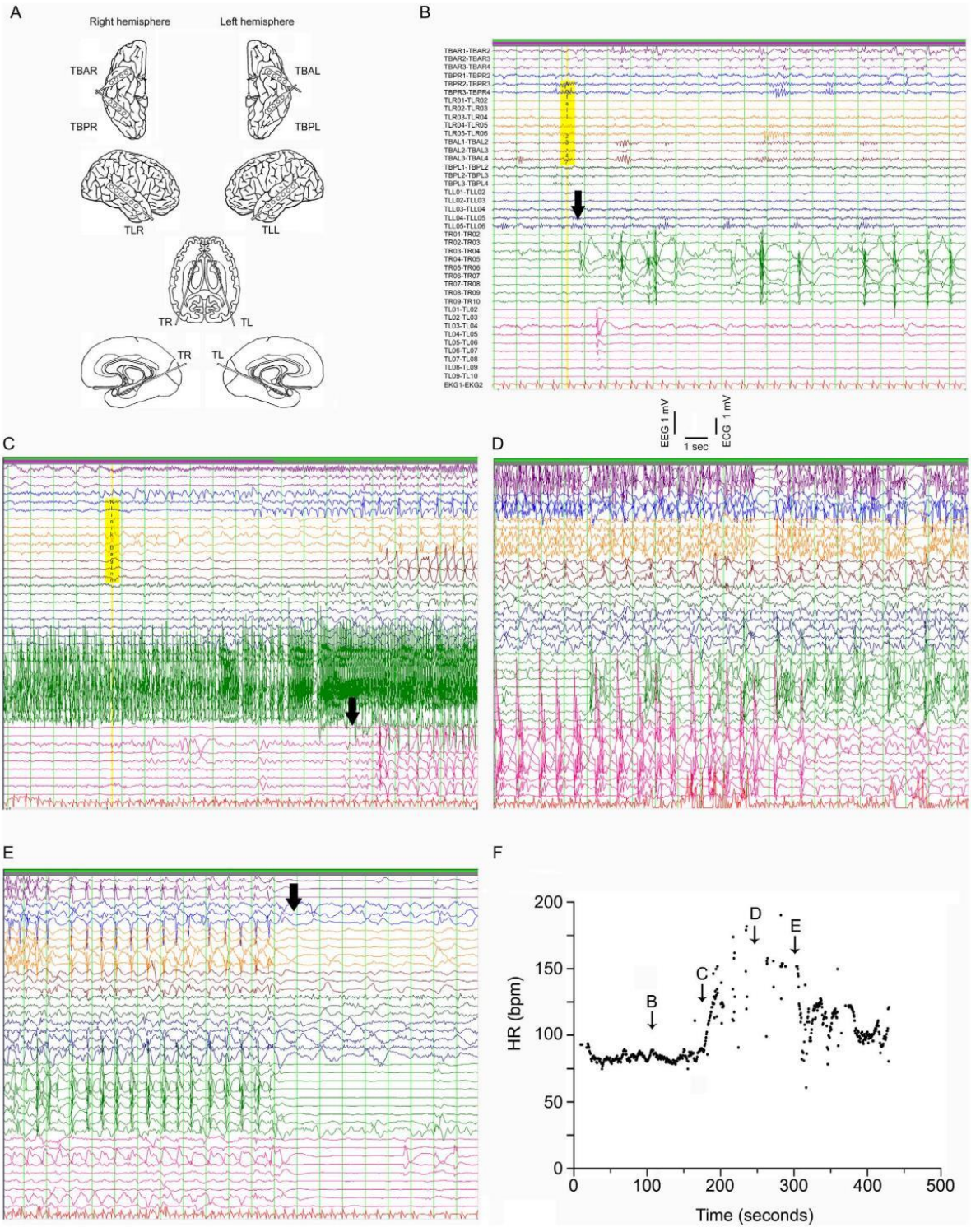

Figure 2. Example of original EEG- and ECG-traces during a focal seizure with right-sided hippocampal onset. (A) Implantation scheme of intracranial electrodes (patient no. 119). (B–E) EEG-traces in bipolar montage (localization as given in panel A, the lower numbers apply to the contacts opposite to the cable outlet of the respective strip or depths electrodes) and ECG-traces (last trace, labeled as EKG1-EKG2, represents derivation Einthoven II with inverted polarity). The time period of the recordings is indicated in panel F. (B) Arrow indicates seizure-onset in the right

hippocampus. (C) The arrow indicates onset of ictal activity in the left hippocampus. (D) Note the compromised ECG trace due to movement artifacts of the patient. (E) The arrow indicates the abrupt termination of seizure activity. (F) Time course of HR during this focal seizure with impaired responsiveness and complex automatisms. The arrows indicate the time periods from which example panels B–E have been selected. Note the missing values after propagation of ictal activity to the left hemisphere (time period between arrows "C" and "E").
doi:10.1371/journal.pone.0064765.g002

seizures of 2 patients. Abnormal QTc shortening occurred only in 1 right hippocampal seizure (Table 3).

No potentially serious periictal cardiac arrhythmias were observed, but only 6 short episodes of ictal or postictal pronounced sinus arrhythmia without consistent association with seizure-onset from one hippocampus.

Discussion

Our study suggests asymmetric seizure-related modulation of cardiac repolarization. There are controversial data on lateralized cerebral representation of cardiac function. Most studies have assessed HR in response to iatrogenic interventions. Studies using pharmacological inactivation of both hemispheres via intracarotid amobarbital injection have produced conflicting data [4,18–20]. Nevertheless, an increase of HR following inactivation of the left hemisphere was observed in all four studies, whereas HR displayed an increase [18,19], a decrease [4] or no significant change [20] upon right-sided inactivation, supporting at least the notion that cortical networks tonically modulate sympathetic and parasympathetic activity. The reasons for this controversy are unclear, but a variable representation and function of the right hemisphere, a region-specific excitatory or inhibitory modulation and different cerebral epileptogenic lesions in these studies may play a role. In

Table 2. Seizure characteristics.

Patient no.	Side of hippocampal seizure activity	Seizure types	Duration* (s)
48	Left	CPS; SGTCS; CPS	180; 184; 113
	Right	CPS; CPS	121; 154
105	Left	SPS; SPS; SPS	118; 132; 137
	Right	SPS; SPS	75; 254
111	Left	CPS; CPS; CPS; CPS	79; 120; 71; 60
	Right	CPS; CPS	37; 38
112	Left	CPS; CPS; CPS	66; 95; 73
	Right	CPS; CPS	87; 47
119	Left	SCP; SCP; SCP	65; 68; 144
	Right	CPS; CPS; CPS	127; 200; 100
127	Left	CPS; CPS; CPS	130; 71;180
	Right	CPS; CPS; CPS	282; 96; 195
132	Left	CPS; CPS;CPS	61; 87; 91
	Right	SPS; SPS; CPS	78; 64; 132
135	Left	SPS; SPS	42; 47
	Right	CPS; CPS; SPS	66; 64; 255
143	Left	CPS; CPS; CPS	102; 115; 67
	Right	SGTCS; CPS	128; 77
144	Left	SPS; CPS	163; 243
	Right	SPS; SPS; SPS	141; 20; 289
160	Left	SPS/CPS#; CPS	101; 120
	Right	CPS; CPS	69; 137
182	Left	CPS; SGTCS; CPS	102; 118; 104
	Right	SCP; SCP; SGTCS; SGTCS	30; 35; 191; 196
184	Left	SPS/CPS#; CPS; SPS	60; 111; 28
	Right	SGTCS; CPS; SCP; SPS	273; 188; 44; 80
187	Left	CPS; CPS;CPS	391; 173; 193
	Right	SCP; SCP; SCP	118; 86; 65
202	Left	CPS; SGTCS	134; 147
	Right	CPS; CPS	188; 143

*According to EEG pattern.
#Consciousness not tested.
CPS, complex-partial seizures; SGTCS, secondarily generalized tonic-clonic seizure; SCP, subclinical EEG pattern (no objective clinical signs apart from alterations of cardiac activity and with or without testing); SPS, simple partial seizure.
doi:10.1371/journal.pone.0064765.t002

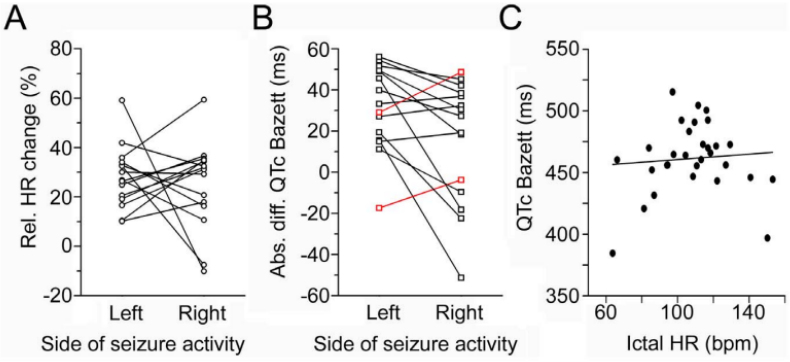

Figure 3. Plot of HR and QTc changes per patient. (A) Relative ictal HR changes and (B) absolute QTc differences using Bazett's formula were plotted separately for each patient and side of seizure activity. Corresponding data pairs from each patient were connected with a line. Note that only in two patients, QTc increased by more than 10 ms during right hippocampal seizures as compared to left hippocampal seizures (B, highlighted in red). (C) Individual QTc values (Bazett) did not correlate with corresponding absolute ictal heart rates (linear regression, $p = 0.67$). Examples were illustrated using Bazett's formula, as this correction formula is known to overestimate corrected QT values, so that a potential artificial bias, if present, should be clearly visible.
doi:10.1371/journal.pone.0064765.g003

another study, electrical stimulation of the insula was performed in 5 patients and shown that a decrease of HR occurred more frequently upon stimulation of the left insula, whereas increase in HR was more often elicited by stimulation of the right insula, suggesting a differential distribution of cardiovascular networks on both hemispheres [3].

In contrast to these studies, we have investigated ECG features in response to spontaneously occurring seizures. It is not surprising that seizure activity within the hippocampus has effects on cardiac function, as a number of anatomical pathways connect the hippocampus and the amygdala with other brain regions known to modulate heart activity (e.g. with the insula and cingulate gyrus or via the Papez circuit with thalamic and hypothalamic projections

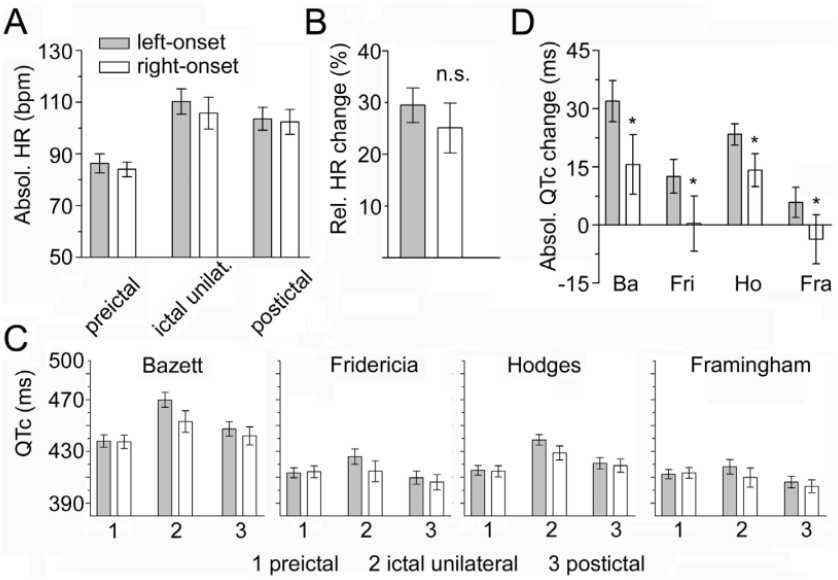

Figure 4. HR and QTc increase with ictal activity, whereupon modulation of QTc, but not of HR, is asymmetrically lateralized. (A) Absolute HR at different timepoints from all patients was averaged (based on a mean HR per timepoint and side of seizure-onset per patient). Paired data for right- (white bars) and left-hippocampal onset (grey bars) were available from all 15 patients at all timepoints. (B) Relative HR changes from all patients were averaged with no significant difference of ictal modulation of HR between left- and right-onset seizures. (C) QT intervals corrected with all four formulas (grey bars, left-hippocampal seizures; white bars, right-hippocampal seizures) were plotted versus three timepoints (1, preictal; 2, unilateral ictal activity; 3, postictal). (D) The absolute ictal changes of QT intervals using all four correction formulas (Ba, Bazett; Fri, Fridericia; Ho, Hodges; Fra, Framingham) were separately plotted for left- (grey bars) and right-hippocampal seizures (white bars). QT lengthening was significantly greater during left-hippocampal activity as assessed with all 4 correction formulas, suggesting an asymmetric ictal modulation of cardiac repolarization. All data expressed as mean±S.E.M.
doi:10.1371/journal.pone.0064765.g004

Table 3. Summary of seizure-related QT alterations.

Abnormal QTc prolongation in all 4 formulas according to Luo et al. 2004*		
	Left-hippocampal seizures (n = 41)	Right-hippocampal seizures (n = 37)
Seizures (no./%)	**7/17.1%**	2/5.4%
Patients (no./%)	**4/26.7%**	2/13.3%
Abnormal QTc prolongation above 500 ms according to Bazett's formula		
	Left-hippocampal seizures (n = 41)	Right-hippocampal seizures (n = 37)
Seizures (no.)	**5/12.2%**	2/5.4%
Patients (no.)	**3/20%**	2/13.3%
Abnormal QTc shortening according to Luo et al. 2004* (using Bazett, Fridericia, Framingham)		
	Left-hippocampal seizures (n = 41)	Right-hippocampal seizures (n = 37)
Seizures (no.)	0/0%	1/2.7%
Patients (no.)	0/0%	1/6.7%
QTc shortening ≤ -10 ms in all 4 formulas		
	Left-hippocampal seizures (n = 41)	Right-hippocampal seizures (n = 37)
Seizures (no.)	2/4.9%	**5/13.5%**
Patients (no.)	2/13.3%	**4/26.7%**

*Luo S, Michler K, Johnston P, Macfarlane PW. A comparison of commonly used QT correction formulae: the effect of heart rate on the QTc of normal ECGs. J Electrocardiol. 2004;37 Suppl: 81–90 (see table S1). In 5 of the 82 included seizures, ictal QT intervals could not been reliably analyzed.
doi:10.1371/journal.pone.0064765.t003

to the brain stem) [1,21]. Capitalizing on a pair-wise comparison, we have found that cardiac repolarization, but not HR, is differentially modulated during limited hippocampal seizure activity of the left and right hemisphere. The lack of laterality in HR regulation is in line with a number of previous studies which have shown that e.g. ictal HR was not correlated with the side of seizure activity and that ictal bradycardia appeared to be associated with bilateral spread of ictal activity, but not with lateralized seizure activity [11,13,22].

The asymmetric cerebral control of cardiac repolarization is supported by a number of human and animal studies investigating QT intervals following neurological injuries [5–7,23]. Importantly, Critchley and co-workers have investigated the cerebral areas involved in the modulation of cardiac activity during mental and physical stress in people without apparent affection of the brain [24]. To that end, they have recorded regional blood flow (as assessed by $H_2{}^{15}O$-PET scans) and simultaneously recorded ECG features during a subtraction task with or without time restriction (mental stress paradigm) and isometric handgrip squeeze under specific conditions (physical stress paradigm). The major findings are that proarrhythmic abnormalities of cardiac repolarization were positively correlated with an asymmetric increase in regional blood flow in the midbrain on the right side, and, at least in one feature of QT abnormality, also in the right parahippocampal gyrus, supporting the notion of an asymmetric representation of the autonomic control of cardiac repolarization including mesiotemporal brain structures. These findings may explain our observation that seizure-related modulation of cardiac repolarization appears to be asymmetrically localized in people with mesial TLE. Accordingly, right- and left-sided hippocampal seizure activity may induce an asymmetric sympathetic modulation of cardiac repolarization via mesiotemporal networks (parahippocampal gyrus) and midbrain networks (via projections to the brain stem). Interestingly, QTc intervals shortened again after the propagation of seizure activity to the contralateral hemisphere, (probably linked to bilateral activation of involved neuronal mesiotemporal and midbrain networks) and returned to baseline postictally (figure S1).

Whereas the above cited studies include patients or animals with a structural lesion due to ischemic stroke or in people during physiologic stress tasks (and without known brain diseases), we have assessed the effects of ongoing abnormal seizure activity in a limited neuronal network. It is tempting to speculate that, in analogy to *positive* clinical signs such as motor activity or somatosensory sensations, seizure activity leads to activation of autonomic cardiac networks. It remains, however, unclear whether pathologic ictal activity has excitatory or inhibitory (disrupting) effects on autonomic networks regulating cardiac repolarization.

Clinical relevance of asymmetric seizure-related modulation of cardiac repolarization.

Cardiac repolarization was assessed as QT intervals corrected with four established formulas to account for selective bias using e.g. Bazett's formula only (which is known to overestimate corrected QT intervals). QTc was not correlated with absolute ictal HR (Figure 3C), suggesting that a major bias by the correction procedure is unlikely. In our study, QTc intervals were lengthened to a greater extent during left hippocampal seizure activity, in average by more than 30 ms (range −17 ms to 56 ms) during left- and by about 15 ms (range −51 ms to 48 ms) during right-sided hippocampal activity, strengthening the hypothesis of side-dependent regulation of cardiac function. This averaged difference in QTc intervals appears to be subtle. At the level of individual seizures, however, abnormal QTc prolongation above normal upper limits was more frequently observed with left hippocampal seizures, whereas abnormal QTc shortening below normal limits was noted in one right-sided seizure only (table 3). The clinical relevance of these findings is not clear at present. They may indicate an increased risk of abnormal ictal QT prolongation in people with left mTLE. This could be especially relevant in the presence of drugs interfering with cardiac repolarization [25]. Seizure-related abnormal prolongation and shortening of QT intervals have recently been described [8–11], could facilitate onset of ventricular tachyarrhythmia and thereby contribute to the

pathophysiology of sudden unexpected death in epilepsy (SUDEP) [26,27]. One established risk factor for SUDEP is the presence of generalized convulsive seizures (GCS), potentially due to GCS-related cardiorespiratory dysfunction [27]. It is of note that abnormal QTc shortening predominantly occurs with GCS [10], providing a possible link between seizure-related pathologic cardiac repolarization and fatal ventricular tachyarrhythmia. In some witnessed SUDEP cases, however, GCS have not been reported or sudden death has occurred in association with an epileptic aura [28]. In this context, our findings may be of particular importance: We have detected seizure-related abnormal QT alterations during ictal activity confined to one hippocampus and temporal lobe, suggesting that even seizures without extended involvement of the brain (such as auras) and without generalized convulsions may bear the risk of sudden cardiac death as one cause for SUDEP.

Study Limitations

This is a retrospective study capitalizing on intracranial EEG recordings. Implantation of electrodes was performed according to an *a-priori* hypothesis of seizure-onset zone based on electro-clinical and MRI findings during non-invasive presurgical assessment with the ultimate goal of using as few electrodes as possible (to minimize potential risks and complications). Therefore, the number of implanted electrodes is limited with a consecutive spatial sampling bias. Ictal activity tends to spread from the hippocampus to lateral and basal parts of the temporal lobe and the insula of the same hemisphere, and later during the seizure, to the contralateral hemisphere as well [29]. In this context, it is important to note that ictal HR appears to increase gradually with regional spreading of ictal activity [30]. Thus, we cannot rule out that at the timepoint where we have assessed RR and QT intervals, ictal activity within the hippocampus has propagated to other, neocortical ipsilateral or contralateral regions of the brain. We have analyzed HR changes in a subgroup of our patients who had additional strip and grid electrodes (figure S2) and found that the extent of relative HR changes (as a rough measure of ictal spread) was in the same range as compared to the data of all patients, suggesting limited seizure activity within the ipsilateral temporal lobe. Another weakness of our study is that we have only analyzed ECG data at arbitrarily selected timepoints (e.g. preictal and postictal values were assessed at a given time interval before and after the seizure, whereas ictal HR was determined where RR intervals were shortest and where 3 consecutive QRS intervals allowed manual measurement of both RR and QT intervals). Thus, we predominantly describe "snapshots" of cardiac activity during seizures, but do not have information on the time course of seizure-related cardiac regulation. It would be interesting to know the entire dynamics of HR and cardiac repolarization during seizures arising from the left and right hemisphere. This question, however, has not been directly addressed in our study. Another important methodical limitation of our study stems from the fact that correction of QT intervals is very complex. Even under steady-state conditions, the relationship between QT and RR intervals is not linear. For instance, when cycle length varies, QT intervals are influenced by changes in the preceding cycle length and by preceding interbeat intervals [31]. These adaptations may take 30 to 120 seconds [31]. Seizure-related HR changes are variable throughout the course of epileptic seizures (Figure 2), e.g. HR can steadily increase and stay on a certain level for some time (e.g. 30 seconds), and then return to baseline again, or display rather rapid alterations with increases, decreases and increase again or vice-versa [15]. Furthermore, seizures usually last for about 30 to 90 seconds. Thus, if the "true" QT values require many seconds or several minutes to be set, our data on corrected QT intervals may be of limited clinical relevance. These difficulties cannot be overcome and are inherent to the paroxysmal nature of epileptic seizures (which represent transient disturbances of the brain activity with a limited duration only). Our study, however, was designed to tackle the question whether there is a difference between left- and right sided seizures within a given patient across several seizures from each side. This means that the inherent limitations apply at least to both conditions (left versus right), which strengthens, to some extent, the relevance of our findings.

A further weakness of our study is the lack of information on periictal respiratory function in our patients, as seizure-related hypoxemia increases the likelihood of both QTc prolongation and shortening [32]. However, ictal apnea appears to be correlated with spread of seizure-activity to the contralateral hemisphere, and not with a particular side of seizure-onset or seizure-lateralization [33], supporting our conclusions on the link between ictal modulation of autonomic networks and alteration of cardiac repolarization. In addition, anticonvulsant drugs such as rufinamide and primidone have been reported to modulate cardiac repolarization [25,34]. Our patients, however, have not been on these drugs during video-EEG telemetry. The strength and the additional value of this study is the comparison of seizures arising from both hippocampi within the same patients, thereby controlling for a great portion of intra-individual variability of cardiovascular and autonomic features and allowing pair-wise analysis of HR and QT intervals. In addition, we have investigated a relatively homogenous study population which may further reduce errors due to lesion type and cerebral localization of the focus as a potential confounder. Importantly, the presence of hippocampal sclerosis *per se* has no measurable effect on the cardiovascular autonomic properties as compared to people with focal epilepsy without hippocampal sclerosis [35]. Using this conservative approach, our study population has undergone a strong selection with a limited final sample size, thereby weakening the statistical power of our study. Despite this high selection, comparison of corrected QT intervals has reached statistically significant differences, strengthening the hypothesis of an asymmetric representation of autonomic networks involved in the regulation of cardiac repolarization.

Supporting Information

Figure S1 QTc decreases after propagation to the contralateral hemisphere.
(DOCX)

Figure S2 Extent of ictal HR changes correlates with spatial spread, but not with duration of ictal activity.
(DOCX)

Table S1 Upper and lower normal limits of normal QTc for 4 correction formulas.
(DOCX)

Acknowledgments

We thank Maria Schruff for help with the patient collection and Dr. Guido Lüchters from the Center for Development Research of the University Bonn for support with statistical analysis.

Author Contributions

Conceived and designed the experiments: RS. Analyzed the data: RS AJ. Wrote the paper: RS. Acquisition of data, statistical analysis and interpretation: RS AJ. Critical revision of the manuscript for important intellectual content: AJ CEE.

References

1. Cheung RT, Hachinski V (2000) The insula and cerebrogenic sudden death. Arch Neurol 57: 1685–1688.
2. Napadow V, Dhond R, Conti G, Makris N, Brown EN et al. (2008) Brain correlates of autonomic modulation: combining heart rate variability with fMRI. Neuroimage 42: 169–177.
3. Oppenheimer SM, Gelb A, Girvin JP, Hachinski VC (1992) Cardiovascular effects of human insular cortex stimulation. Neurology 42: 1727–1732.
4. Zamrini EY, Meador KJ, Loring DW, Nichols FT, Lee GP et al. (1990) Unilateral cerebral inactivation produces differential left/right heart rate responses. Neurology 40: 1408–1411.
5. Sander D, Klingelhöfer J (1995) Changes of circadian blood pressure patterns and cardiovascular parameters indicate lateralization of sympathetic activation following hemispheric brain infarction. J Neurol 242: 313–318.
6. Colivicchi F, Bassi A, Santini M, Caltagirone C (2004) Cardiac autonomic derangement and arrhythmias in right-sided stroke with insular involvement. Stroke 35: 2094–2098.
7. Tatschl C, Stöllberger C, Matz K, Yilmaz N, Eckhardt R et al. (2006) Insular involvement is associated with QT prolongation: ECG abnormalities in patients with acute stroke. Cerebrovasc Dis 21: 47–53.
8. Brotherstone R, Blackhall B, McLellan A (2010) Lengthening of corrected QT during epileptic seizures. Epilepsia 51: 221–232.
9. Surges R, Adjei P, Kallis C, Erhuero J, Scott CA et al. (2010) Pathologic cardiac repolarization in pharmacoresistant epilepsy and its potential role in sudden unexpected death in epilepsy: a case-control study. Epilepsia 51: 233–242.
10. Surges R, Scott CA, Walker MC (2010) Enhanced QT shortening and persistent tachycardia after generalized seizures. Neurology 74: 421–426.
11. Moseley BD, Wirrell EC, Nickels K, Johnson JN, Ackerman MJ et al. (2011) Electrocardiographic and oximetric changes during partial complex and generalized seizures. Epilepsy Res 95: 237–245.
12. Leutmezer F, Schernthaner C, Lurger S, Pötzelberger K, Baumgartner C (2003) Electrocardiographic changes at the onset of epileptic seizures. Epilepsia 44: 348–354.
13. Britton JW, Ghearing GR, Benarroch EE, Cascino GD (2006) The ictal bradycardia syndrome: localization and lateralization. Epilepsia 47: 737–744.
14. Kawai M, Goldsmith IL, Verma A (2006) Differential effects of left and right hemispheric seizure onset on heart rate. Neurology 66: 1279–1280.
15. Panchani J, Adjei P, Henneberger C, Scott CA, Thompson AJ et al. (2011) Asymmetric hemispheric representation of periictal heart rate modulation is individually lateralised. Epileptic Disord 13: 172–176.
16. Aytemir K, Maarouf N, Gallagher MM, Yap YG, Waktare JE, Malik M (1999) Comparison of formulae for heart rate correction of QT interval in exercise electrocardiograms. Pacing Clin Electrophysiol 22: 1397–1401.
17. Luo S, Michler K, Johnston P, Macfarlane PW (2004) A comparison of commonly used QT correction formulae: the effect of heart rate on the QTc of normal ECGs. J Electrocardiol 37 Suppl: 81–90.
18. Jokeit H, Noerpel I, Herbord E, Ebner A (2000) Heart rate does not decrease after right hemispheric amobarbital injection. Neurology 54: 2347–2348.
19. Ahern GL, Sollers JJ, Lane RD, Labiner DM, Herring AM et al. (2001) Heart rate and heart rate variability changes in the intracarotid sodium amobarbital test. Epilepsia 42: 912–921.
20. Hilz MJ, Dütsch M, Perrine K, Nelson PK, Rauhut U et al. (2001) Hemispheric influence on autonomic modulation and baroreflex sensitivity. Ann Neurol 49: 575–584.
21. Leung H, Schindler K, Kwan P, Elger C (2007) Asystole induced by electrical stimulation of the left cingulate gyrus. Epileptic Disord 9: 77–81.
22. Opherk C, Coromilas J, Hirsch LJ (2002) Heart rate and EKG changes in 102 seizures: analysis of influencing factors. Epilepsy Res 52: 117–127.
23. Hachinski VC, Oppenheimer SM, Wilson JX, Guiraudon C, Cechetto DF (1992) Asymmetry of sympathetic consequences of experimental stroke. Arch Neurol 49: 697–702.
24. Critchley HD, Taggart P, Sutton PM, Holdright DR, Batchvarov V et al. (2005) Mental stress and sudden cardiac death: asymmetric midbrain activity as a linking mechanism. Brain 128: 75–85.
25. Surges R, Taggart P, Sander JW, Walker MC (2010) Too long or too short? New insights into abnormal cardiac repolarization in people with chronic epilepsy and its potential role in sudden unexpected death. Epilepsia 51: 738–744.
26. Espinosa PS, Lee JW, Tedrow UB, Bromfield EB, Dworetzky BA (2009) Sudden unexpected near death in epilepsy: malignant arrhythmia from a partial seizure. Neurology 72: 1702–1703.
27. Surges R, Sander JW (2012) Sudden unexpected death in epilepsy: mechanisms, prevalence, and prevention. Curr Opin Neurol 25: 201–207.
28. Langan Y, Nashef L, Sander JW (2000) Sudden unexpected death in epilepsy: a series of witnessed deaths. J Neurol Neurosurg Psychiatry 68: 211–213.
29. Spencer SS, Williamson PD, Spencer DD, Mattson RH (1987) Human hippocampal seizure spread studied by depth and subdural recording: the hippocampal commissure. Epilepsia 28: 479–489.
30. Epstein MA, Sperling MR, O'Connor MJ (1992) Cardiac rhythm during temporal lobe seizures. Neurology 42: 50–53.
31. Franz MR, Swerdlow CD, Liem LB, Schaefer J (1988). Cycle length dependence of human action potential duration in vivo. Effects of single extrastimuli, sudden sustained rate acceleration and deceleration, and different steady-state frequencies. J Clin Invest 82: 972–979.
32. Seyal M, Pascual F, Lee CY, Li CS, Bateman LM (2011) Seizure-related cardiac repolarization abnormalities are associated with ictal hypoxemia. Epilepsia 52: 2105–2111.
33. Seyal M, Bateman LM (2009) Ictal apnea linked to contralateral spread of temporal lobe seizures: Intracranial EEG recordings in refractory temporal lobe epilepsy. Epilepsia 50: 2557–2562.
34. Schimpf R, Veltmann C, Papavassiliu T, Rudic B, Göksu T et al. (2012) Drug-induced QT-interval shortening following antiepileptic treatment with oral rufinamide. Heart Rhythm 9: 776–781.
35. Ansakorpi H, Korpelainen JT, Tanskanen P, Huikuri HV, Koivula A et al. (2004) Cardiovascular regulation and hippocampal sclerosis. Epilepsia 45: 933–939.

Supplementary information

A methodical weakness of our study is the fact that in 6 of our 15 patients, data interpretation is limited due to a spatial sampling bias, as those patients had bilateral hippocampal electrodes only (Figure 1A, table 1). In 7 patients, however, depths electrodes were placed within the hippocampus as well as additional strip and grid electrodes on lateral and basal parts of the temporal lobe on both sides, allowing correlation of HR change and spatial spread of ictal activity. ECG signals were analyzed 1 min before seizure onset, after unilateral hippocampal onset (at the timepoint where HR was highest and before spread to other regions than ipsilateral hippocampus), after spread to ipsilateral neocortical areas (regional) and after spread to contralateral hemisphere (hippocampus or neocortical electrodes). In line with previous reports [Epstein et al., 1992], we have observed that the extent of ictal HR changes depends on the degree of spatial spread, but not on the duration of ictal activity (supplementary figure).

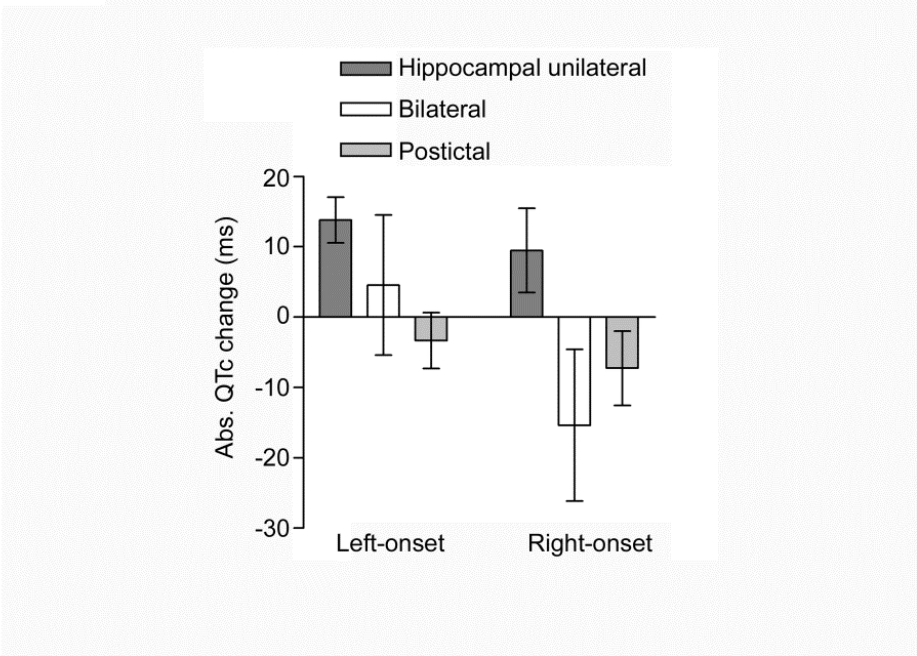

Figure S1. QTc decreases after propagation to the contralateral hemisphere.

Absolute QTc changes (using Fridericia's formula) were plotted during unilateral hippocampal activity, after propagation to the contralateral hemisphere (bilateral hippocampal seizure activity) and after seizure cessation (postictal) for each hemisphere. QTc increased with unilateral seizure activity and decreased after propagation to the contralateral hemisphere, with a more pronounced decrease with seizures displaying a right-

onset. Data available for 11 patients and left-onset seizures, and 9 patients and right-onset seizures.

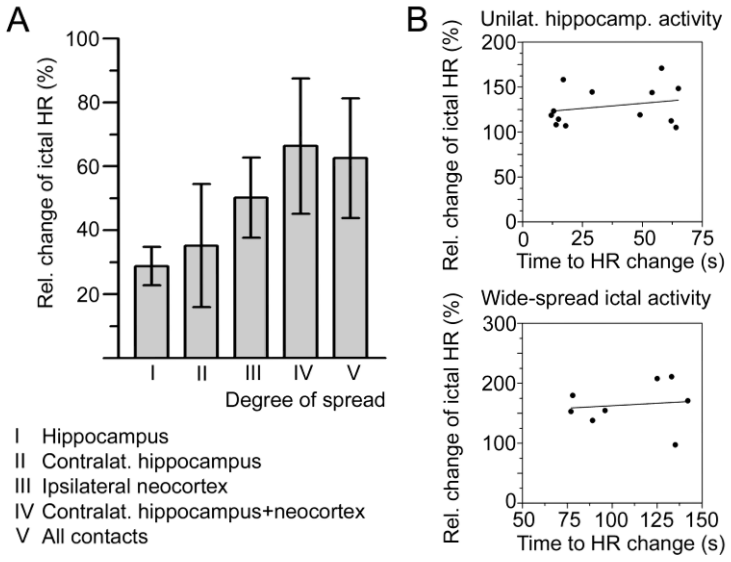

Figure S2. Extent of ictal HR changes correlates with spatial spread, but not with duration of ictal activity.

(A) HR changes relative to preictal values were plotted versus the spatial spread (from focal hippocampal activity to wide-spread ictal activity covering all available intracranial contacts; indicated as I-V). Two seizures per patient (only of those 7 patients who had hippocampal depths electrodes and additional strip or grid electrodes covering the temporal lobe on both sided) were included (one with right, one with left-sided hippocampal onset). Final number of included data points (from left bar to right bar): 14, 4, 5, 3 and 5. Data expressed as mean±S.E.M. (B) Relative change of ictal HR was plotted versus the time interval between EEG-onset and timepoint of HR assessment at two ictal phases: during unilateral hippocampal activity (upper panel; linear regression p=0.44) and during wide-spread ictal activity (with additional ictal activity in the contralateral hippocampus and neocortex or in all available contacts; lower panel, p=0.79).

Table S1. Upper and lower normal limits of normal QTc for 4 correction formulas.

Adapted from Luo et al., (2004) A comparison of commonly used QT correction formulae: the effect of heart rate on the QTc of normal ECGs. J Electrocardiol 37 Suppl: 81-90.

	Upper normal limits (98%, in ms)				
Gender	**HR (bpm)**	**QTcB**	**QTcFri**	**QTcFra**	**QTcH**
Both	All HR	483	460	457	457
	HR < 60	454	459	459	466
	HR 60 to 99	483	461	458	456
	HR > 99	492	445	436	451
Male	All HR	480	457	454	454
	HR < 60	450	455	455	465
	HR 60 to 99	480	457	454	452
	HR > 99	490	445	436	450
Female	All HR	486	463	461	460
	HR < 60	460	463	463	470
	HR 60 to 99	486	465	462	459
	HR > 99	492	448	434	452
	Lower normal limits (2%, in ms)				
Gender	**HR (bpm)**	**QTcB**	**QTcFri**	**QTcFra**	**QTcH**
Both	All HR	378	365	368	372
	HR < 60	363	372	367	375
	HR 60 to 99	382	370	374	372
	HR > 99	380	343	350	371
Male	All HR	374	361	364	369
	HR < 60	361	368	363	369
	HR 60 to 99	379	368	372	369
	HR > 99	378	341	348	369
Female	All HR	386	369	372	377
	HR < 60	372	381	377	386
	HR 60 to 99	388	374	378	376
	HR > 99	389	350	354	374

Epilepsy Research 157 (2019) 106187

Contents lists available at ScienceDirect

Epilepsy Research

journal homepage: www.elsevier.com/locate/epilepsyres

Semi-automatic quantification of seizure-related effects on heart activity

Arthur Jordan[a,b,1], Marcel Bausch[a,1], Rainer Surges[a,*]

[a] Department of Epileptology, University Hospital Bonn, Bonn, Germany
[b] Department of Neurology, University Hospital of Aachen, Aachen, Germany

ARTICLE INFO

Keyword:
HR analysis

ABSTRACT

Objective: : Seizure-related modulation of heart rate (HR) was examined extensively in previous studies. However, the overall effect on HR attributable to epileptic seizures is difficult to determine, given the considerable fluctuations of HR before and during seizures. Here, we developed a semi-automatic procedure allowing quantification of the total impact of seizures on HR and determination of temporal relationships between seizure onset assessed by intracranial EEG (iEEG) and ECG.

Methods: : ECG and iEEG data of epilepsy patients undergoing video-EEG telemetry for epilepsy surgery with bilateral hippocampal depth electrodes were analysed retrospectively. Consecutive RR intervals and HR profiles were determined using R detection algorithms. Novel features including the normalized ictal area under the curve (niAUC), as well as the time point of ECG onset (HR breakpoint) were calculated. Selected HR features were compared to widely-used manually acquired measures. Data are given as median ± SD.

Results: : Fifteen patients had a total of 34 seizures with left-hippocampal and 37 seizures with right-hippocampal onset. HR increased by 9 ± 19% during seizures. Latency between iEEG seizure-onset to the HR breakpoint was 23 ± 22 s. No significant difference between left- and right-hippocampal seizures was observed with respect to HR increases, latencies and niAUC. A comparison between results of the semi-automatic and manual approach revealed that ictal HR changes showed a higher correlation (r = 0.6) than niAUC (r = 0.4).

Conclusions: : The proposed semi-automatic approach to analyze continuous HR data provides useful tools for estimating the overall effect of seizures on HR in greater detail. Our results suggest that the side of hippocampal seizure onset has no significant effect on the latency and extent of ictal HR changes. The algorithms may be of further use in clinical research and the development of seizure detection devices.

1. Introduction

Brain regions involved in the autonomic nervous system (ANS) can be affected during epileptic seizures, resulting in a variety of autonomic symptoms. Previous studies analysed features of HR with regard to their localizing and lateralizing value in people with epilepsy (Britton et al., 2006; Garcia et al., 2001; Kawai et al., 2006; Leutmezer et al., 2003; Moseley et al., 2011; Panchani et al., 2011). Ictal tachycardia (ITC) occurs frequently, either as a consequence of excessive movement or due to spread of seizure activity into regions of the central ANS. ITC appears to occur more frequently in seizures of temporal lobe origin (Garcia et al., 2001; Weil et al., 2005). Ictal bradycardia, albeit far less prevalent, is of greater clinical interest due to its hemodynamic consequences (Britton et al., 2006; Hampel et al., 2017; Reeves et al., 1996). Recent studies also examined temporal relationships between EEG seizure onsets and ECG changes with potential relevance for closed-loop intervention systems based on HR (Hirsch et al., 2015; Leutmezer et al., 2003).

Most previous studies have capitalized on threshold-based detection of seizure-related HR changes which are limited by the fact that this approach usually does not take the entire duration of the seizure into account. Moreover, individual thresholds are often selected arbitrarily for each seizure or patient despite the existence of established thresholds such as 100 bpm for ITC and 60 bpm for ictal bradycardia. In a recent study we investigated whether ictal HR modulation depends on the hemisphere of seizure-onset (Surges et al., 2013). Since a quantitative approach was required, we captured maximum deviations from a pre-ictal reference HR snapshot under the assumption that the maximal or minimal HR deflection from a pre-ictal baseline value adequately reflects the overall degree of influence the seizure has on cardiac action. Because of EMG and movement artifacts, HR was sampled manually ("manual max method"). Similar approaches were also chosen in

* Corresponding author at: Department of Neurology, University Hospital RWTH Aachen, Pauwelsstr. 30, 52074 Aachen, Germany.
E-mail address: ajordan@ukaachen.de (A. Jordan).
[1] These authors contributed equally to this work.

https://doi.org/10.1016/j.eplepsyres.2019.106187
Received 23 April 2019; Received in revised form 21 July 2019; Accepted 11 August 2019
Available online 12 August 2019
0920-1211/

previous studies by other authors in epilepsy research as well as in treadmill exercise studies (Jouven et al., 2005; Nashef et al., 1996; Opherk et al., 2002; Zijlmans et al., 2002).

While the manual max method is a measure of the maximal extent to which HR is altered after seizure onset, it does not consider any other HR changes over the entire course of the seizure, which upon closer inspection often follow complex dynamics and therefore likely contain valuable information about the overall impact a seizure may have on the ANS. Here, we developed and applied novel measures of ictal HR analysis to characterize seizure-related effects on HR in greater detail. Furthermore, we analysed latencies between EEG seizure-onset to ECG breakpoint (Hirsch et al., 2015; Kato et al., 2014; Stefanidou et al., 2015).

2. Materials, methods and patient collective

2.1. Patients

Video-EEG data of patients with medically refractory mesial temporal lobe epilepsy undergoing presurgical video-EEG monitoring between January 2000 and December 2011 in the Department of Epileptology at the University Hospital Bonn (Germany) were reviewed retrospectively. Since this study is a retrospective audit of EEG and ECG data collected during clinical procedures, informed patient consent was not required. The study was approved as such by the local medical ethics committee (Ethikkommission an der Medizinischen Fakultät der Rheinischen Friedrich-Wilhelms-Universität Bonn). The patient group and electrophysiological data analysed in this study were already reported in one of our previous studies (Surges et al., 2013). All patients were implanted with bilateral hippocampal depth electrodes and had at least 2 recorded seizures with independent onset from each hippocampus. A summary of the clinical details is given in Table 1.

2.2. Manual EEG and ECG analysis

EEG data acquisition was performed with a Stellate Harmonie digital video-EEG system (Version 5.4, Schwarzer GmbH/Natus, Germany) using up to 128 channels, a 200 Hz sampling rate and a 16-bit analog-to-digital converter. Data were band pass filtered between 0.016 and 70 Hz. ECG recordings were acquired simultaneously with iEEG from a modified lead-I configuration. The main prerequisite for ictal HR analysis is the identification of iEEG seizure onset and propagation time of seizure activity to the contralateral hemisphere, which was done manually by reviewing iEEG data with particular focus on the bilateral hippocampal depth electrodes. The iEEG seizure onset separates the pre-ictal and ictal periods both for the manual and the semi-automatic method. The criteria for a typical seizure of hippocampal origin are onset with low amplitude fast activity (LAFA) or hypersynchronous discharges (Alarcon et al., 1995; Engel Jr, 2001) and the modulation of frequency and amplitude of the discharges as the seizure progresses. The occurrence of such ictal activity in the EEG electrodes of the contralateral hemisphere in the further course of the seizure was considered as propagation phenomenon, which was defined as the end of unilateral activity. The HR analysis was limited to the time interval before seizure onset until the time point of seizure propagation to the contralateral hemisphere. To rule out the influence of contralateral seizure activity on HR as accurately as possible, only the time interval between seizure onset and propagation was analysed whenever a propagation was present.

The objective of the manual max method was to get an estimate of the effect of seizure activity on the central ANS by measuring HR in ictal ECG recordings at predefined time points in a manual and therefore artifact-immune manner. In order to obtain the pre-ictal "baseline" value for the manual method, four consecutive RR intervals at a fixed one minute interval prior to seizure onset were measured within the Stellate Harmonie EEG analysis environment and their mean was calculated. For the ictal value the same approach was applied at the moment of maximum HR deviation from the pre-ictal value, which can be towards lower as well as towards higher HR. The maximum deviation was considered and chosen in order to normalize the recording and to allow comparison across all analysed seizures. In addition, the number of seizures during which HR exceeded 100 bpm (which is commonly defined as tachycardia) was determined. Another approach to explore effects of the EEG seizure onset on HR is to analyze ictal HR changes relative to individual baseline values. We therefore defined a significant HR increase as an increase of the ictal median HR of 2 SD above the pre-ictal median HR. This approach, however, requires a semi-automatic ECG analysis, which is described in the next section.

2.3. Semi-automatic ECG analysis

In order to obtain continuous HR profiles across the entire peri-ictal interval, all seizure recordings were exported in ASCII .txt format from the Stellate software and the ECG channels and analysed using custom MATLAB (version R2011a) scripts. Two different algorithms were used for R detection: the first one was developed by LIBROW™ (Chernenko, 2007) and the second one is a MATLAB implementation of the widely known Pan Tompkins algorithm (Sedghamiz, 2014). Results of both algorithms were compared manually for each seizure and results with greater number of outliers and distorted areas were rejected. Recordings that could not be assessed with either of the two algorithms due to insufficient signal to noise ratio (SNR) were discarded. Because of this manual review, this approach is referred to as "semi-automatic". A custom filter has been developed to remove artifacts and inaccuracies in the HR profiles, caused by motion and EMG noise in the underlying ECG data. Outliers in the HR profiles are detected by calculating the difference between each data point of the raw HR profile and its convoluted version and marking data points that lie outside the 1% bounds of the probability density function of these differences. The MATLAB code for the filter can be reviewed in the filterHRprofile function in the supplementary section.

These continuous HR profiles were used to calculate the pre-ictal baseline, median ictal HR, pre-ictal and ictal AUC as well as the latency to significant HR changes. The median of all instantaneous pre-ictal HR values (60/RR in seconds) prior to the seizure onset in iEEG constitutes the baseline. This baseline value is therefore not to be confused with the manually determined baseline. It is depicted as the grey horizontal line in Fig. 3. The median of all HR values during the time interval where seizure activity in iEEG is limited to the onset hemisphere constitutes the "automatic median value", which is shown in Fig. 3 as the purple (short) horizontal line. Medians were chosen because they are less sensitive to outliers caused by residual R detection artifacts. HR data in the time intervals after electroencephalographic spread of seizure activity to the contralateral hemisphere is less relevant for our lateralization analyses, however its relationship with the latency to seizure propagation was examined. For this analysis the median HR for the time interval between the propagation and seizure cessation was calculated. Seizures with a duration of less than 10 s prior to being detectable in the contralateral hemisphere were also discarded. In order to examine the amount of false positive HR increases we split the original baseline interval into two halves, the first of which we consider to represent the non-peri-ictal period and the second of which constitutes the immediate baseline interval (immediately preceding the seizure). A false positive HR increase is detected if in a dataset the median HR of the non-peri-ictal period exceeds 2 SD of the half of the baseline interval immediately preceding the seizure onset.

In order to calculate the normalized ictal AUC (niAUC) a continuous function for smoothening was approximated for each HR profile by convolving the HR data with a gaussian kernel and interpolating the data points removed by the artifact filter, by means of spline interpolation. The area between the smoothened HR graph and the pre-ictal baseline was calculated for a pre-ictal and ictal interval by means of

Table 1
Clinical details and analysed seizures of patients.

Patient no.	Sex	Age*/Epilepsy duration*/ handedness	MRI finding	Surgery	Intracranial electrodes	Seizure onset	Seizure type	Duration*
48	M	32/32/R	Bilat. HS	No	Hipp: 1 depth electrode (10 c.) on each side from posterior ExHipp: None	Left-hippocampal	CPS	180 s
							SGTCS	184 s
						Right-hippocampal	CPS	113 s
							CPS	121 s
							CPS	154 s
105	M	39/3/R	Bilat. HS R > L	No	Hipp: 1 depth electrode (10 c.) on each side from posterior ExHipp: None	Left-hippocampal	SPS	118 s
							SPS	132 s
						Right-hippocampal	SPS	137 s
							SPS	75 s
							SPS	254 s
111	M	28/23/L	HS L	SAHE L	Hipp: 1 depth electrode (10 c.) on each side from posterior ExHipp: 1 temporo-lateral (16 c.) and 2 temporo-basal (4 c.) strip electrodes on left side	Left-hippocampal	CPS	79 s
							CPS	120 s
							CPS	71 s
						Right-hippocampal	CPS	60 s
							CPS	37 s
							CPS	38 s
112	F	24/4/R	Bilat. HS L > R	No	Hipp: 1 depth electrode (10 c.) on each side from posterior ExHipp: 1 temporo-lateral (4 c.) and 2 temporo-basal (4 c.) strip electrodes on each side	Left-hippocampal	CPS	66 s
							CPS	95 s
						Right-hippocampal	CPS	73 s
							CPS	87 s
							CPS	47 s
119	F	55/33/R	Bilat. HS L > R	SAHE R	Hipp: 1 depth electrode (10 c.) on each side from posterior ExHipp: 1 temporo-lateral (6 c.) and 2 temporo-basal (4 c.) strip electrodes on each side	Left-hippocampal	SCP	65 s
							SCP	68 s
						Right-hippocampal	SCP	144 s
							CPS	127 s
							CPS	200 s
							CPS	100 s
127	M	45/39/L	None	No	Hipp: 1 depth electrode (10 c.) on each side from posterior ExHipp: 1 temporo-lateral (4 c.) and 2 temporo-basal (4 c.) strip electrodes on each side	Left-hippocampal	CPS	130 s
							CPS	71 s
						Right-hippocampal	CPS	180 s
							CPS	282 s
							CPS	96 s
							CPS	195 s
132	F	47/7/R	Bilat. HS	No	Hipp: 1 depth electrode (10 c.) on each side from posterior ExHipp: None	Left-hippocampal	CPS	61 s
							CPS	87 s
						Right-hippocampal	CPS	91 s
							SPS	78 s
							SPS	64 s
							CPS	132 s
135	F	46/33/R	HS R	SAHE R	Hipp: 1 depth electrode (10 c.) on each side from posterior ExHipp: 1 temporo-lateral (6 c.) and 2 temporo-basal (4 c.) strip electrodes on each side	Left-hippocampal	SPS	42 s
						Right-hippocampal	SPS	47 s
							CPS	66 s
							CPS	64 s
							SPS	255 s
143	M	22/15/L	None	SAHE L	Hipp: 1 depth electrode (10 c.) on each side from posterior ExHipp: 2 temporo-basal (4 c.) strip electrodes on each side 1 temporo-lateral strip electrode (6 c.) on right side and 1 grid electrode (32 c.) on left side covering Wernicke's area	Left-hippocampal	CPS	102 s
							CPS	115 s
						Right-hippocampal	CPS	67 s
							SGTCS	128 s
							CPS	77 s

(*continued on next page*)

Table 1 (*continued*)

Patient no.	Sex	Age*/Epilepsy duration+/ handedness	MRI finding	Surgery	Intracranial electrodes	Seizure onset	Seizure type	Duration+
144	F	35/30/R	Bilat. HS L > R	No	Hipp: 1 depth electrode (10 c.) on each side from posterior ExHipp: None	Left-hippocampal	SPS	163 s
						Right-hippocampal	CPS	243 s
							SPS	141 s
							SPS	20 s
							SPS	289 s
160	F	31/30/R	Bilat. HS	TL-resection incl. AHE L	Hipp: 1 depth electrode (10 c.) on each side from posterior ExHipp: None	Left-hippocampal	SPS/CPS#	101 s
						Right-hippocampal	CPS	120 s
							CPS	69 s
							CPS	137 s
182	F	34/14/R	Bilat. HS L > R	No	Hipp: 1 depth electrode (10 c.) on each side from posterior ExHipp: None	Left-hippocampal	CPS	102 s
							SGTCS	118 s
						Right-hippocampal	CPS	104 s
							SCP-	30 s
							SCP-	35 s
							SGTCS	191 s
							SGTCS	196 s
184	F	28/25/L	HS R	No	Hipp: 2 depth electrodes (8 c.) on each side from lateral ExHipp: 2 temporo-basal (4 c.) strip electrodes on each side	Left-hippocampal	SPS/CPS#	60 s
							CPS	111 s
						Right-hippocampal	SPS	28 s
							SGTCS	273 s
							CPS	188 s
							SCP	44 s
							SPS	80 s
187	F	31/29/R	Bilat. HS	No	Hipp: 1 depth electrode (10 c.) on each side from posterior ExHipp: 1 temporo-lateral (6 c.) and 2 temporo-basal (4 c.) strip electrodes on each side	Left-hippocampal	CPS	391 s
							CPS	173 s
						Right-hippocampal	CPS	193 s
							SCP	118 s
							SCP	86 s
							SCP	65 s
202	M	28/15/R	HS L	No	Hipp: 5 depths electrodes (10 c.) on each side from lateral ExHipp: 2 frontal strip electrodes (8 c.) on each side	Left-hippocampal	CPS	134 s
						Right-hippocampal	SGTCS	147 s
							CPS	188 s
							CPS	143 s

c, electrode contacts; ExHipp, extrahippocampal; Hipp, hippocampal; HS, hipppocampal sclerosis; L, left; R, right; SAHE, selective amygdala-hippocampectomie; TL, temporal lobe; CPS, complex-partial seizures; SGTCS, secondarily generalized tonic-clonic seizure; SCP, subclinical EEG pattern (no objective clinical signs apart from alterations of cardiac activity and with or without testing); SPS, simple partial seizure.

* At telemetry.

\+ According to EEG pattern.

\# Consciousness not tested.

\- Excluded from semiautomatic analysis due to insufficient signal-to-noise-ratio.

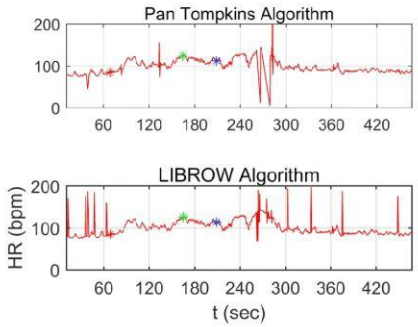

Fig. 1. R detection algorithms differently perform with ECG recordings containing artifacts. In this case, the result of the LIBROW algorithm was chosen and processed further. A left hippocampal seizure, recorded on patient 187 (as in Figure 3 and 2 D). The asterisks mark relevant timepoints, as assessed by EEG review. Red – beginning of unilateral seizure activity, green – propagation to the contralateral hemisphere, blue – cessation of the seizure.

trapezoidal numerical integration as implemented in MATLAB's trapz function. The ictal AUC is the area in the time interval between the seizure onset in iEEG and seizure cessation or spread to the contralateral hemisphere. This exact measure is visualized in Fig. 3 as the red area. The pre-ictal AUC (not shown in Fig. 3) constitutes the area under the smoothened HR graph and the pre-ictal baseline but for a time interval of equal length to the ictal interval to normalize for time. Its ending is marked by the iEEG seizure onset. The pre-ictal AUC was subtracted from the ictal AUC to obtain the final niAUC value, which is higher in case pre-ictal HR is below baseline HR and lower in case pre-ictal HR is higher than the baseline. niAUC therefore represents the effect of the EEG seizure onset on HR and is at the same time a measure for the cumulative effect on unilateral seizure activity on HR.

Computation of the HR breakpoint was accomplished by a novel statistical algorithm which detects HR increases greater than 1 SD above the pre-ictal baseline and with certain duration over a minimal time interval. This minimal time interval is also derived from the pre-ictal HR data by determining the number of consecutive values being greater than 1 SD. After random permutation of all pre-ictal instantaneous HR values, this process is repeated 10.000 times. Finally, the length of the largest of 10.000 "snippets" of consecutive HR values greater than 1 SD constitutes this minimal time interval. The beginning of the minimal time interval is defined as the ECG or HR breakpoint. The MATLAB code was made available in the calculateOnset function in the supplementary section.

2.4. Statistics

The distribution of the data was tested using the one-sample Kolmogorov-Smirnov test. For calculation of p-values in the lateralization analysis, a two-sided Wilcoxon rank sum test was performed, and data are given as medians ± SD and visualized as medians ± S.E.M. P values < 0.05 were considered statistically significant. MATLAB (versions R2011a and R2016b) was used to implement both the statistical analysis, as well as data visualisation.

3. Results

In 15 patients, 11 seizures out of a total of 82 had to be discarded entirely due to low SNR. Thirty-four left-sided and 37 right-sided hippocampal seizures were of sufficient signal quality to undergo further analysis. The performance of the two different R detection algorithms differed considerably when ECG artifacts were present in the recordings (Fig. 1). Overall, the LIBROW algorithm has proven to be more robust in analyzing the given datasets, failing to provide superior HR profiles in 3 seizures only, whereas the Pan Tompkins algorithm failed to deliver correct ECG analysis results in 9 seizures.

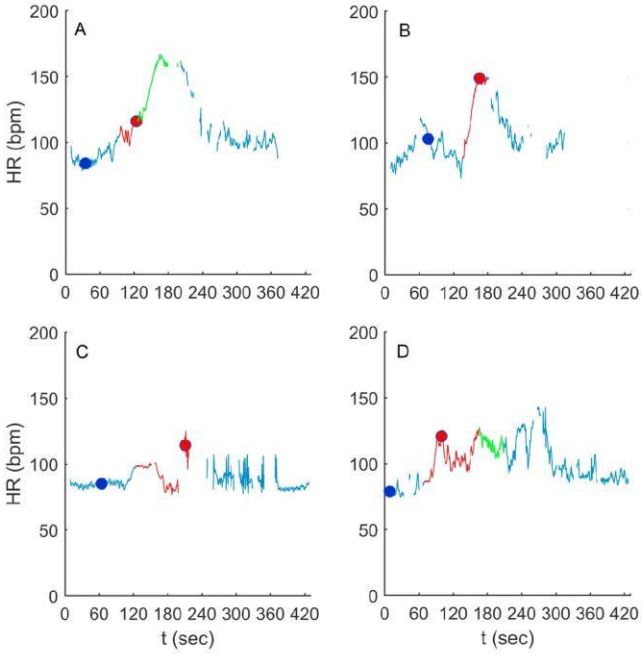

Fig. 2. Peri-ictal heart rate in temporal lobe epilepsy shows strong intraindividual as well as interindividual fluctuations. Automatic data after artifact removal, plotted alongside with the according manual data. Red graph: seizure activity limited to side of onset. Green graph: seizure activity propagated to the contralateral hemisphere. Blue circle: manual pre-ictal measurement. Red circle: manual ictal max measurement. **(A)** Patient 111, left-hippocampal seizure: steady increase in HR, which precedes EEG seizure onset. **(B)** Patient 111, right-hippocampal seizure without propagation to the contralateral electrodes with significant pre-ictal HR fluctuations. **(C)** Patient 202, left-hippocampal seizure without propagation with HR decrease. Residual artifacts are present. **(D)** Patient 187, left-hippocampal seizure with step-wise HR increase.

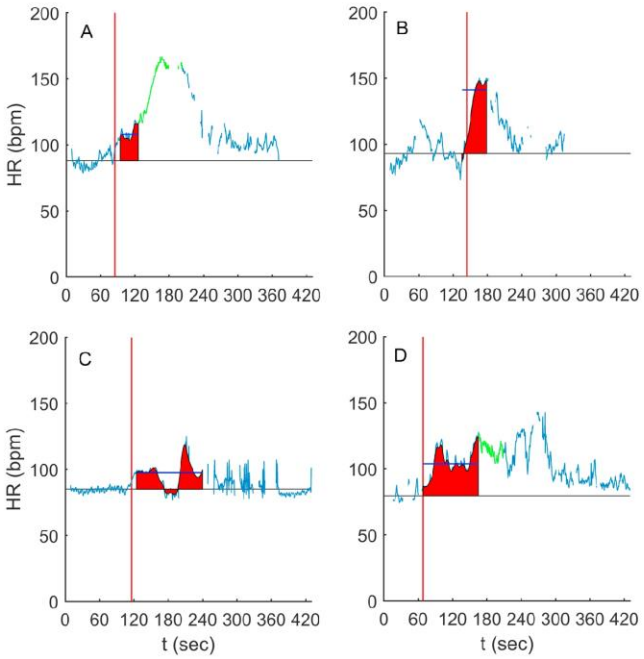

Fig. 3. Summary of all HR features, applied to the examples from Figure 2. Vertical red line: HR breakpoint, as calculated by the novel algorithm. Grey horizontal line: median pre-ictal HR (baseline). Red area: ictal AUC, calculated for the entire unilateral ictal interval under the spline interpolated (smoothened) curve. Seizure onset as determined by EEG is marked by the left bound of the red AUC. The right bound of the red AUC marks seizure cessation or propagation to the contralateral hemisphere (also beginning of the green graph). Purple (short) horizontal line: unilateral ictal HR median. Note: in **(A)** and **(C)** the HR breakpoint, as calculated by the HR breakpoint detection algorithm, precedes the EEG onset.

Importantly, hippocampal seizures display a very variable HR over time (Fig. 2). The semi-automatic analysis revealed local maxima and minima in the HR profile throughout the ictal period as well as during the pre-ictal phase in all seizures. Likewise, the duration of unilateral seizure activity shows a great variability (58 ± 63 s, range: 10–230 s). These results suggest that a more detailed semi-automatic analysis is superior to a manual investigation of seizure-related HR changes by selecting near-instantaneous HR derived from 4 consecutive RR intervals only. A semi-automatic analysis also allows determination of various other features.

A summary of novel peri-ictal HR features, as applied to the HR profiles is shown in Figure 3. The median of all pre-ictal HR values serves as a solid baseline allowing normalization of ictal AUC and relative ictal HR changes (see Fig. 3, horizontal lines). Furthermore, the HR breakpoint detection algorithm has proven to be very reliable in detecting significant HR changes (see Fig. 3, vertical red lines). The automatically detected HR breakpoint was delayed by 16 ± 22 s as compared to EEG seizure onset (Fig. 3 B), whereas in some seizures, the HR breakpoint preceded the EEG onset (Figs. 3 A and C). In 9 seizures, the latency from EEG seizure onset to HR breakpoint was greater than the duration of unilateral seizure activity. These seizures were excluded from the latency analysis.

In a next step, we investigated whether seizures with left-hippocampal onset were different from seizures with right-hippocampal onset with respect to these novel ECG features. In 91% of left-hippocampal and 70% of right-hippocampal seizures, HR transiently exceeded 100 bpm while still being limited to the onset hemisphere which might suggest that ictal tachycardia is more common in left-hippocampal seizures. However, in 21% (n = 7) of left and 28% (n = 9) of right hippocampal seizures HR exceeded 100 bpm throughout the pre-ictal interval. Fifty percent of left-sided and 54% of right-sided seizures displayed a significant heart rate increase of 2 SD above pre-ictal baseline. Six out of 71 seizures exhibited such false positive increases in HR and less than 10% of heart beats fell outside 2 SD of the immediate baseline interval (Supplementary Figure 3). Among simple partial seizures (SPS) the percentage of significant HR increases was the lowest (25 and 41% for left and right respectively) and among secondary generalized tonic-clonic seizures 67 vs. 75% displayed a significant increase (Supplementary Figure 1). No significant difference between left and right onset seizures was found ($p = 0{,}24$). No cases of ictal bradycardia (i.e. HR < 60 bpm or HR lower than 2 SD below the pre-ictal median) were observed. Fifty-four seizures occurred at daytime and 17 have been recorded during nocturnal period. We can observe a significant difference in baseline HR during nighttime (71.4 bpm ± 14 vs. 85.3 bpm ± 14), which was defined as the time period between 10:00 p.m. to 6:00 a.m. ($p = 0.0017$). No significant difference in absolute HR increase (11bpm ± 12 vs. 8bpm ± 13, $p = 0.24$) was observed between night and day (Supplementary Figure 2). In total 37 (21 left and 16 right-hemispheric onset) seizures propagated to the contralateral hemisphere. The median duration until propagation was 42 s (± 38 s Range 10–213 s). The median HR after propagation was 125 bpm (± 21 bpm range: 78–164 bpm). Median post-propagation HR was 124 bpm for left-sided and 140 bpm for right-sided seizures. Over all seizures the absolute change of post-propagation HR compared to the pre-ictal baseline shows a weak positive correlation ($r = 0.0789$, $p = 0.6426$) to the duration until seizure propagation occurs. Similarly, the correlation between the duration until seizure propagation and the median HR during unilateral seizure activity is non-significant ($r = 0.0903$, $p = 0.5950$). A comparison of pre-ictal and ictal HR values in left and right hippocampal seizures from the automatically computed data over the entire time intervals, as in manual measurements, revealed no significant lateralization effect ($p = 0.95$ and $p = 0.55$, Fig. 4 A). Comparisons of neither normalized ictal AUC nor latencies to seizure onset revealed significant differences between seizures with right and left-hippocampal onset ($p = 0.92$ and $p = 0.58$, Fig. 4 B and C). Surprisingly, increases of HR determined by the HR breakpoint detection algorithm preceded the apparent EEG seizure onset in 24% (n = 9, 8.5 ± 2.9 s) of left hippocampal seizures and in 11% (n = 4,

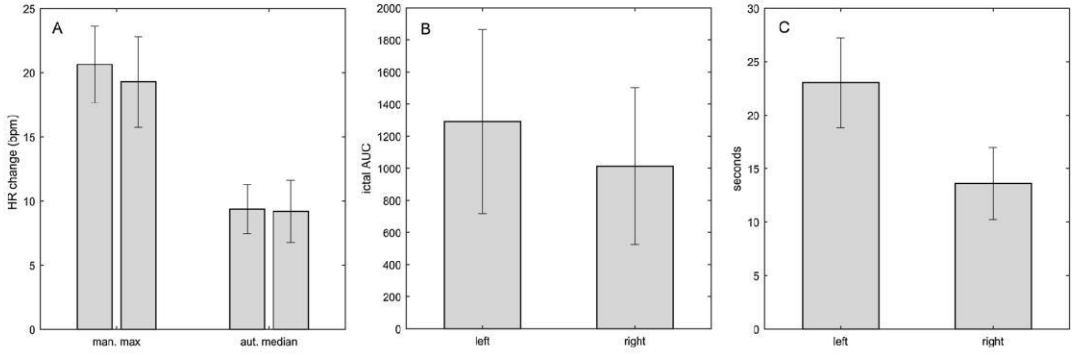

Fig. 4. Analysis of hemispheric lateralization. No significant lateralization effects are evident in any of the described HR features in the underlying data. Each bar represents the median of the underlying HR feature values across 34 left or 37 right onset hippocampal seizures ± S.E.M. **(A)** Comparison of the manual max method with the automatically calculated median across all ictal HR values. As expected, median max values are higher, however they fail to represent the time variable and can induce artificial effects. **(B)** Comparison of median niAUC in left vs. right-hippocampal seizures. **(C)** Comparison of latencies between iEEG seizure onset and the HR breakpoint, as calculated by the breakpoint detection algorithm.

4.7 ± 1.9 s) of right hippocampal seizures. Out of 12 seizures with HR breakpoints preceding the iEEG onset we found 1 seizure with 2/s slow waves in the corresponding hippocampal depth electrodes, whereas the rest featured either LAFA (n = 1) or hypersynchronous spikes (n = 11). Irregular iEEG patterns are not over-represented among seizures with premature HR breakpoints.

Finally, we compared the characteristics of the manually determined seizure-related HR to ECG features extracted by semi-automatic analysis. While the manual max method appears to be reasonably well-suited for determination of the median ictal HR (Fig. 5 A, r = 0.6), it does not reliably predict the niAUC (r = 0.4) (Fig. 5 B).

4. Discussion

The aims of this study were to develop a more objective, accurate and precise approach for seizure-related HR analysis and to apply it to continuous HR data recorded in a highly selected patient group to test the value of HR as a lateralizing sign in TLE.

4.1. Methodical considerations

As a baseline for the manual max method, one pre-ictal snapshot was chosen at a fixed time point. Pre-ictal HR can display significant fluctuations, thereby distorting the baseline. Due to the short time interval being sampled, no accurate estimation of pre-ictal HR variability is possible. Moreover, our results show that several HR maxima can be present throughout the course of the seizure. In some studies, besides maximal HR deflections from the baseline, several HR samples were taken at fixed time points, which might account for ictal HR fluctuations to a better degree (Garcia et al., 2001; Moseley et al., 2011). Median ictal and pre-ictal HR are features which incorporate all pre-ictal and ictal RR intervals, which represent, at least to some extent, the

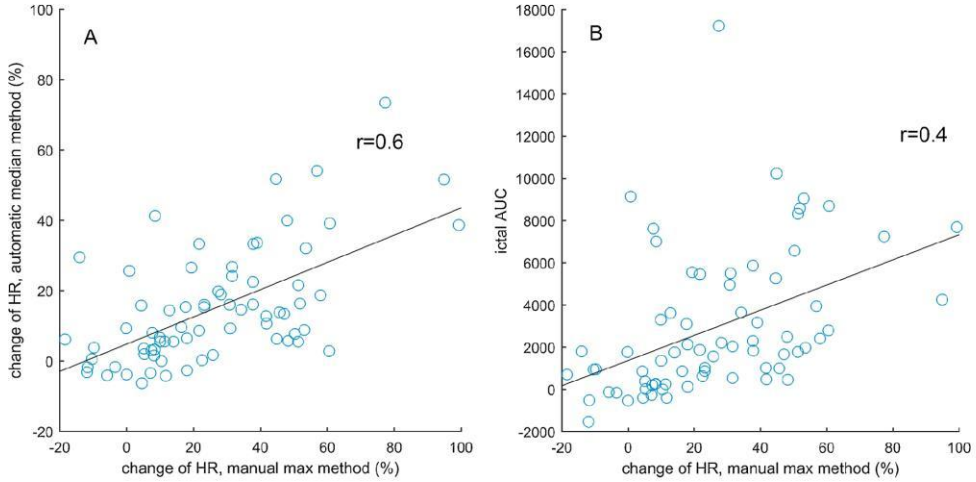

Fig. 5. Taking "HR snapshots" correlates less to niAUC than to the median ictal HR. **(A)** Each data point represents the relative HR change in the manual max method as well as the automatic median method. A significant correlation is to be expected here. **(B)** Correlation of the niAUC with the relative HR change in the manual max method. With the time variable having a greater influence on the ictal AUC, the correlation with the manual "snapshots" becomes less pronounced.

variability over time and which are rather robust against artifacts. Therefore, we decided to include this rather conservative feature into our analyses as a reference. A better representation of the time variable is achieved by calculating niAUC. Ictal AUC without the normalization would constitute a measure for the total amount of additional heartbeats induced by seizures. The normalization considers HR changes shortly before iEEG seizure onset and therefore corrects for them, resulting in the niAUC, which reflects the HR changes taking place solely due to iEEG seizure onset. We also addressed the question how well niAUC and relative HR changes as assessed by the novel semi-automatic approach are predicted by the manual max method. The correlations (Fig. 5) show that niAUC is less well predicted by the manual approach, suggesting that the manual approach fails to give a sufficient estimate of the total impact that seizures exert on HR.

Pronounced alterations of HR during seizures may be of great clinical interest, as ictal bradycardia can progress into asystole (Devinsky, 2004; Schuele et al., 2007) and ITC can be accompanied by altered atrioventricular conduction as well as atrial and ventricular extrasystoles, possibly raising the risk for fatal arrhythmia (22–24). ITC is commonly defined as HR greater than 100 (Hirsch et al., 2015) or 120 bpm (Britton et al., 2006), HR increases greater than 20% (Hirsch et al., 2015; Stefanidou et al., 2015) or HR being greater than the 98th percentile (Moseley et al., 2011). Leutmezer et al. defined ITC as HR being greater than 1 SD of median pre-ictal HR of all patients in the considered group. Our results show that artificial effects can result from choosing different ITC definitions. Since peri-ictal HR shows intra-individual as well as inter-individual variability which must be accounted for, we would consider the 98th percentile or 2 SD definition of ITC as the most suitable for future studies. For the overwhelming majority of seizures less than 10% of heart beats fell outside 2 SD of the immediate baseline interval. Unfortunately the available datasets only represented the peri-ictal period which only had an overall duration in the order of a few minutes. While this data is suitable for examining several aspects of HR dynamics shortly before, during and after a seizure onset and addressing the question of an asymmetrical representation of peri-ictal HR modulation, it cannot show how often the HR falsely exceeded 2 SD of a floating baseline calculated well outside of the ictal/immediate pre-ictal period. For the development of seizure detection systems based on HR dynamics knowing this false positive rate of tachycardia detections is crucial, since a high number of false alarms would not be acceptable to most patients and caregivers. Including accelerometry data might help to differentiate between ictal HR increases and HR increases due to physical activity. In our patient collective, we also observed a correlation of HR with clinical severity of the seizure (SPS vs. CPS vs. GTCS) which was to be expected. No significant difference in absolute HR increase was observed between night and day suggesting that sleep-wake-cycles do not modulate the influence of seizures on HR.

In view of variable nature of peri-ictal HR, analysis of continuous HR data is necessary. Using two different R detection algorithms can increase the number of successfully analysed ECG datasets due to individual strengths and weaknesses of each algorithm. In most of our datasets, filtering of the HR profiles was required. Interpolation of the resulting “gaps” by means of spline interpolation was mandatory for calculating the niAUC, since a continuous function is necessary for trapezoidal numerical integration. These two steps can be omitted if HR profiles do not contain noteworthy amounts of artifacts. Calculation of pre-ictal and ictal median HR does not require interpolation.

To our knowledge, this study is the first to assess niAUC in HR profiles. Leutmezer and colleagues investigated HR dynamics with respect to the EEG seizure onset and found that HR at the time of seizure onset typically displays two ways of rising (Leutmezer et al., 2003). Our data suggest that in the further course of the seizure, HR dynamics vary to a greater extent. Several different patterns, as depicted in Figs. 2 and 3, are possible. In some cases, HR decreases after an initial increase (Figure 3 and 2 C) or shows a step-wise increase (Figure 3 and 2 D). niAUC represents these variations, however caution is advised with ECG data with low SNR. Excessive amounts of artifacts in the resulting HR profiles, as well as large spline interpolated intervals can distort the integrals. HR breakpoints in peri-ictal HR profiles were determined in previous studies with different techniques (Di Gennaro et al., 2004; Leutmezer et al., 2003; Van Elmpt et al., 2006; Kato et al., 2014). The present semi-automatic approach based on MATLAB algorithms provides additional helpful tools, which iare provided as open source files.

In summary, a thorough analysis of continuous HR profiles adds to our understanding of seizure-related HR modulation. This step allows for quantification of peri-ictal as well as ictal fluctuations, calculation of mean or median HR over greater time intervals and finally makes the calculation of features such as HR breakpoint and niAUC possible. While HR breakpoints make latency measurements possible, niAUC is a measure of the cumulative effect of seizure activity on HR and thereby directly or indirectly on the central ANS.

4.2 Does modulation of HR depend on the hemisphere of seizure-onset?

In our highly selected patient group with seizures independently arising from hippocampi of both hemispheres, we did not observe differences on any HR feature irrespective of the applied method. Our findings are in line with a number of previous studies, suggesting that the side of seizure-onset does not influence peri-ictal HR modulation (Epstein et al., 1992; Garcia et al., 2001; Hampel et al., 2017; Keilson et al., 1987; Moseley et al., 2011; Opherk et al., 2002; Rugg-Gunn et al., 2004; Schernthaner et al., 1999), while other studies found evidence for asymmetric effects depending on the hemisphere (Jouven et al., 2005; Kawai et al., 2006).

Di Gennaro et al. investigated latencies from surface EEG onset to HR changes in seizures of temporal lobe origin, reporting no significant difference between left and right (Di Gennaro et al., 2004). Kato and colleagues performed a study suggesting that right mesial temporal lobe seizures have earlier tachycardia onsets (Kato et al., 2014). A similar approach of detecting the HR breakpoint as in our study was applied. However, the EEG seizure onsets in their investigation were detected using surface EEG and the patient group only included patients with seizures arising in one hemisphere. Hirsch et al. analyzed temporal relationships between the seizure onset of ITC, defined as either HR greater than 100 bpm or 20% of a baseline value (Hirsch et al., 2015). They reported longer latencies to ITC in left-hemispheric seizures, however, with an underrepresentation of right-hemispheric seizures. In their collective ictal tachycardia never preceded the iEEG seizure onset. Stefanidou et al. performed an intracranial EEG study, showing that laterality at seizure onset did not predict the occurrence of ITC and that bilateral seizure onset is associated with early tachycardia (Stefanidou et al., 2015).

In our patient group, each patient had seizures arising from both hemispheres independently and the seizure onsets were detected from hippocampal depth electrodes. Importantly, we included 34 left-hippocampal and 37 right-hippocampal seizures in our analysis, which is a well-balanced ratio of right to left and we ruled out influences of the contralateral hemisphere as accurately as possible. We did not observe significant hemisphere-differential effects on latency to the HR breakpoint. The median latency in right-onset seizures appeared to be slightly shorter as compared to left-onset seizures, but the HR breakpoint preceded the apparent seizure-onset as assessed by iEEG in a greater proportion of left-onset seizures. The observation that HR started to rise before apparent electroencephalographic seizure onset might be explained with inaccuracies in iEEG seizure-onset detection caused by subjective bias of the examiners, spatial sampling bias of the limited number of intracranial EEG electrodes or by inaccurate determination of the HR breakpoint. We do not regard the fact that in the study by Hirsch et al. ictal tachycardia was never observed prior to iEEG seizure onsets as a contradiction to our results, because the HR breakpoint is a phenomenon that usually occurs before HR reaches 100bpm or 20% HR increase above baseline. In view of most previous studies and our present results, we believe that the temporal relationships between (i)

EEG seizure onset and HR breakpoint as well as the magnitude of HR changes are of little use as a lateralizing sign in temporal lobe epilepsy and that a putative hemispherical effect, if present, is not clinically meaningful.

5. Conclusions

We have developed a novel MATLAB based approach which allows a semi-automatic analysis of the total impact of seizures on HR and provides novel HR features that may be useful in future automatic seizure detection techniques based on HR measurements. The main analytical methods have been made public in the form of MATLAB script files. The time course of HR during temporal lobe seizures arising from the hippocampus is very variable and does not depend on the side of seizure-onset.

Funding

This research did not receive any specific grant from funding agencies in the public, commercial, or not-for-profit sectors.

Declaration of Competing Interest

A. Jordan and M. Bausch have no financial disclosure to make. R. Surges has received speaker fees or honorary for serving on the advisory board from Bial, Cyberonics, Desitin, Eisai, LivaNova, Novartis and UCB Pharma.

Appendix A. Supplementary data

Supplementary material related to this article can be found, in the online version, at doi:https://doi.org/10.1016/j.eplepsyres.2019.106187.

References

Alarcon, G., Binnie, C.D., Elwes, R.D.C., Polkey, C.E., 1995. Power spectrum and intracranial EEG patterns at seizure onset in partial epilepsy. Electroencephalogr. Clin. Neurophysiol. 94, 326–337.

Britton, J.W., Ghearing, G.R., Benarroch, E.E., Cascino, G.D., 2006. The ictal bradycardia syndrome: localization and lateralization. Epilepsia 47, 737–744.

Chernenko, S., 2007. ECG Processing — R-peaks Detection — Librow — Software [WWW Document]. http://www.librow.com/cases/case-2.

Devinsky, O., 2004. Effects of seizures on autonomic and cardiovascular function. Epilepsy Curr. 4, 43–46.

Di Gennaro, G., Quarato, P.P., Sebastiano, F., Esposito, V., Onorati, P., Grammaldo, L.G., Meldolesi, G.N., Mascia, A., Falco, C., Scoppetta, C., 2004. Ictal heart rate increase precedes EEG discharge in drug-resistant mesial temporal lobe seizures. Clin. Neurophysiol. 115, 1169–1177.

Engel Jr, J., 2001. Mesial temporal lobe epilepsy: what have we learned? Neuroscientist 7, 340–352.

Epstein, M.A., Sperling, M.R., O'connor, M.J., 1992. Cardiac rhythm during temporal lobe seizures. Neurology 42, 50.

Garcia, M., D'Giano, C., Estelles, S., Leiguarda, R., Rabinowicz, A., 2001. Ictal tachycardia: its discriminating potential between temporal and extratemporal seizure foci. Seizure 10, 415–419.

Hampel, K.G., Thijs, R.D., Elger, C.E., Surges, R., 2017. Recurrence risk of ictal asystole in epilepsy. Neurology 10.1212/WNL. 0000000000004266.

Hirsch, M., Altenmüller, D.-M., Schulze-Bonhage, A., 2015. Latencies from intracranial seizure onset to ictal tachycardia: a comparison to surface EEG patterns and other clinical signs. Epilepsia 56, 1639–1647.

Jouven, X., Empana, J.-P., Schwartz, P.J., Desnos, M., Courbon, D., Ducimetière, P., 2005. Heart-rate profile during exercise as a predictor of sudden death. N. Engl. J. Med. 352, 1951–1958.

Kato, K., Jin, K., Itabashi, H., Iwasaki, M., Kakisaka, Y., Aoki, M., Nakasato, N., 2014. Earlier tachycardia onset in right than left mesial temporal lobe seizures. Neurology 83, 1332–1336.

Kawai, M., Goldsmith, I.L., Verma, A., 2006. Differential effects of left and right hemispheric seizure onset on heart rate. Neurology 66, 1279–1280. https://doi.org/10.1212/01.wnl.0000208519.40986.fb.

Keilson, M.J., Hauser, W.A., Magrill, J.P., Goldman, M., 1987. ECG abnormalities in patients with epilepsy. Neurology 37, 1624.

Leutmezer, F., Schernthaner, C., Lurger, S., Pötzelberger, K., Baumgartner, C., 2003. Electrocardiographic changes at the onset of epileptic seizures. Epilepsia 44, 348–354.

Moseley, B.D., Wirrell, E.C., Nickels, K., Johnson, J.N., Ackerman, M.J., Britton, J., 2011. Electrocardiographic and oximetric changes during partial complex and generalized seizures. Epilepsy Res. 95, 237–245.

Nashef, L., Walker, F., Allen, P., Sander, J.W., Shorvon, S.D., Fish, D.R., 1996. Apnoea and bradycardia during epileptic seizures: relation to sudden death in epilepsy. J. Neurol. Neurosurg. Psychiatry 60, 297–300.

Opherk, C., Coromilas, J., Hirsch, L.J., 2002. Heart rate and EKG changes in 102 seizures: analysis of influencing factors. Epilepsy Res. 52, 117–127.

Panchani, J., Adjei, P., Henneberger, C., Scott, C.A., Thompson, A.J., Diehl, B., Walker, M.C., Surges, R., 2011. Asymmetric hemispheric representation of periictal heart rate modulation is individually lateralised. Epileptic Disord. 13, 172–176.

Reeves, A.L., Nollet, K.E., Klass, D.W., Sharbrough, F.W., So, E.L., 1996. The ictal bradycardia syndrome. Epilepsia 37, 983–987.

Rugg-Gunn, F.J., Simister, R.J., Squirrell, M., Holdright, D.R., Duncan, J.S., 2004. Cardiac arrhythmias in focal epilepsy: a prospective long-term study. Lancet 364, 2212–2219.

Schernthaner, C., Lindinger, G., Pötzelberger, K., Zeiler, K., Baumgartner, C., 1999. Autonomic epilepsy–the influence of epileptic discharges on heart rate and rhythm. Wien. Klin. Wochenschr. 111, 392–401.

Schuele, S.U., Bermeo, A.C., Alexopoulos, A.V., Locatelli, E.R., Burgess, R.C., Dinner, D.S., Foldvary-Schaefer, N., 2007. Video-electrographic and clinical features in patients with ictal asystole. Neurology 69, 434–441.

Sedghamiz, H., 2014. Complete Pan Tompkins Implementation ECG QRS Detector - File Exchange - MATLAB Central [WWW Document]. http://de.mathworks.com/matlabcentral/fileexchange/45840-complete-pan-tompkins-implementation-ecg-qrs-detector.

Stefanidou, M., Carlson, C., Friedman, D., 2015. The relationship between seizure onset zone and ictal tachycardia: an intracranial EEG study. Clin. Neurophysiol. 126, 2255–2260.

Surges, R., Jordan, A., Elger, C.E., 2013. Ictal modulation of cardiac repolarization, but not of heart rate, is lateralized in mesial temporal lobe epilepsy. PLoS One 8, e64765.

Van Elmpt, W.J., Nijsen, T.M., Griep, P.A., Arends, J.B., 2006. A model of heart rate changes to detect seizures in severe epilepsy. Seizure 15, 366–375.

Weil, S., Arnold, S., Eisensehr, I., Noachtar, S., 2005. Heart rate increase in otherwise subclinical seizures is different in temporal versus extratemporal seizure onset: support for temporal lobe autonomic influence. Epileptic Disord. Int. Epilepsy J. Videotape 7, 199–204.

Zijlmans, M., Flanagan, D., Gotman, J., 2002. Heart rate changes and ECG abnormalities during epileptic seizures: prevalence and definition of an objective clinical sign. Epilepsia 43, 847–854.

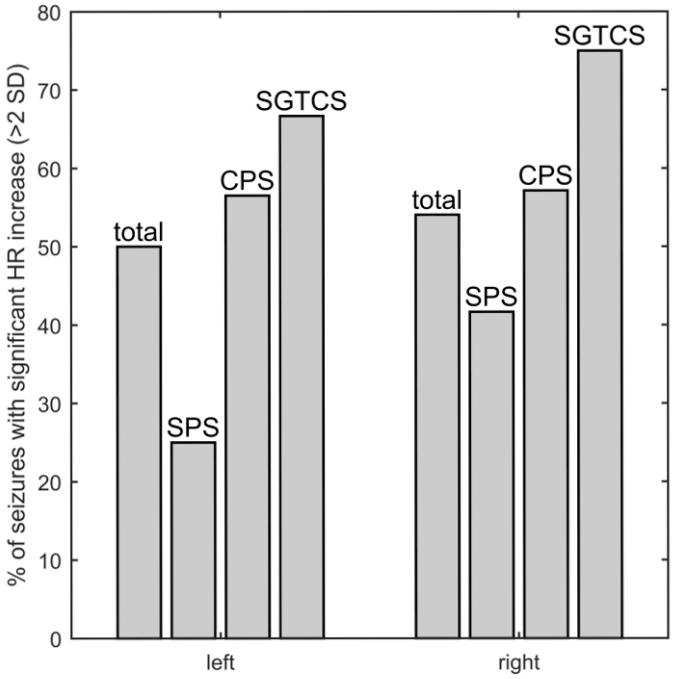

Supp. Fig 1. Significant HR increases occur more frequently in clinically more severe seizures. Each bar corresponds to the percentage of seizures with significant ictal HR increase (> 2SD of baseline HR) among different seizure types in the automatic median method study. Despite only including HR data during unilateral seizure activity, the effect of the seizure type on the extent of ictal HR increase is evident. Overall seizure count left vs. right: 8 vs.12 simple partial seizures (SPS), 23 vs. 21 complex partial seizures (CPS) and 3 vs. 4 secondary generalized tonic-clonic seizures (SGTCS).

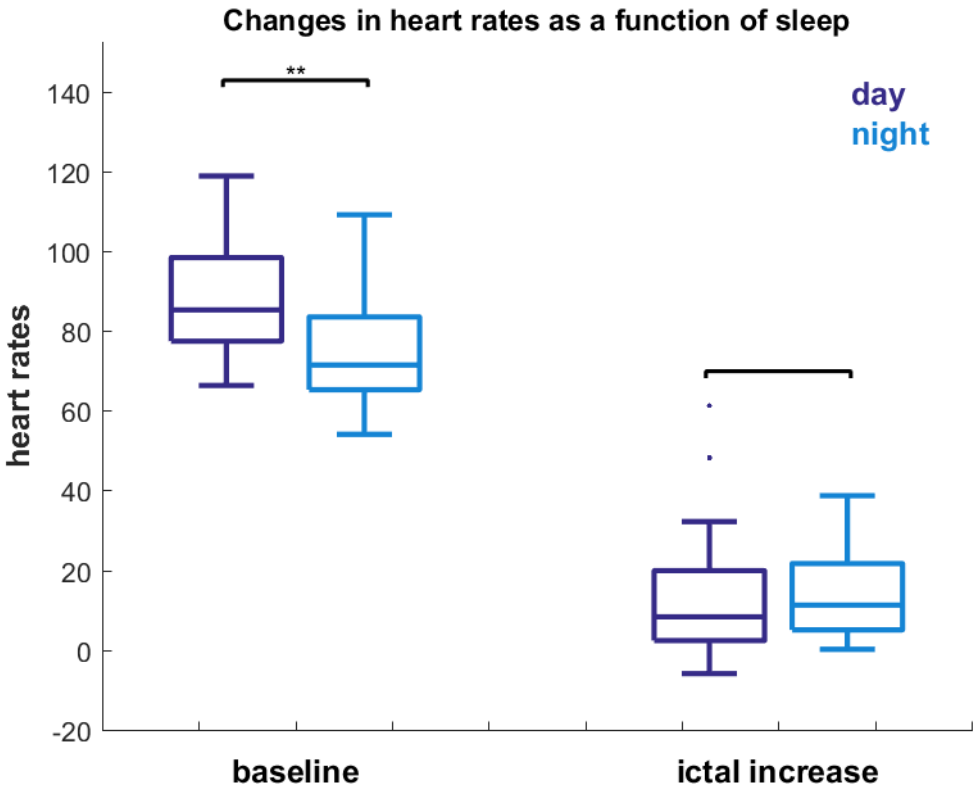

Supp. Fig. 2, Baseline HR, but not the absolute ictal HR increase is significantly different during nighttime. Median baseline HR is significantly lower during nighttime in light blue vs daytime in violet (71.4bpm ± 14 vs. 85.3 bpm ±14, left two boxes). No significant difference in absolute HR increase (11bpm ±12 vs. 8bpm ± 13, p= 0.24) was observed between night and day (right two boxes). Sleep-wake-cycles seem to have no significant effects on the extent of HR change despite lower baselines at night.

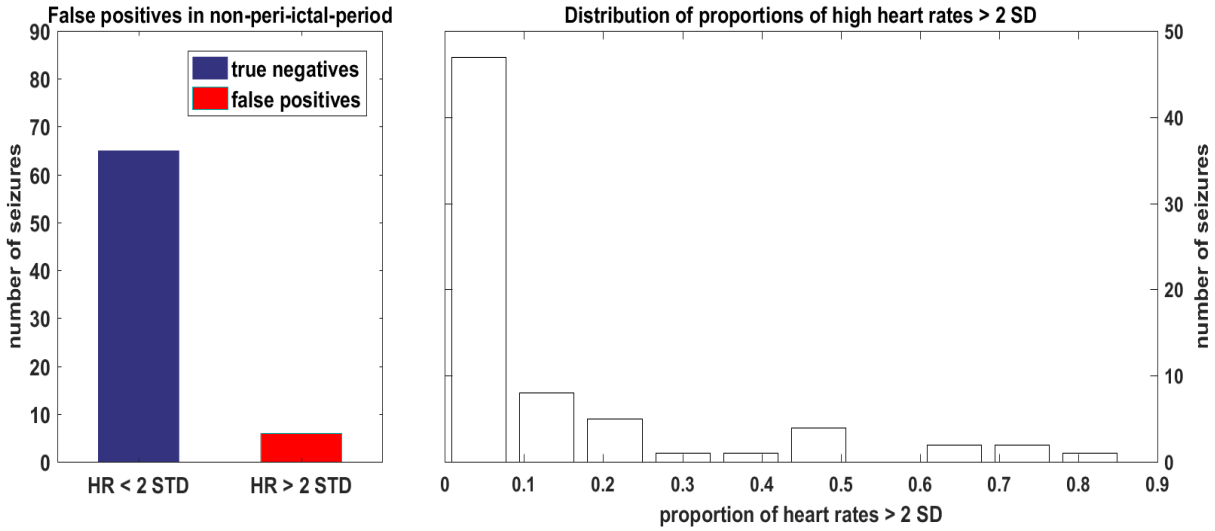

Supp. Fig. 3: Only 6 out of 71 seizures exhibited false positive increases in heart rates. The left subplot shows the number of seizures with a median heart rate during the non-peri-ictal period exceeding that of the immediate baseline interval by two standard deviations ("false positives" for "HR > 2 SD"). The right subplot depicts the proportion of heart rates within the non-peri-ictal period that exceeded the immediate baseline interval by 2 SD for all seizures. For most seizures less than 10 % of heart beats fell outside 2 SD of the immediate baseline interval.

Clinical Neurophysiology 131 (2020) 2932–2933

Contents lists available at ScienceDirect

Clinical Neurophysiology

journal homepage: www.elsevier.com/locate/clinph

Letter to the Editor

Modulation of ictal heart rate is individually lateralized in temporal lobe epilepsy

We read with great interest the case report of Yanai and colleagues in which they present a patient with pharmaco-resistant temporal lobe epilepsy (TLE) undergoing intracranial video-EEG monitoring (Yanai et al., 2020). A total of 7 seizures with right temporal and 8 seizures with left temporal lobe onset were recorded; simultaneous electrocardiographic (ECG) recordings allowed determination of the latency time (LT) between seizure onset and significant heart rate (HR) increase (2 standard deviations higher than baseline HR), the absolute and relative maximal HR increase as compared to pre-ictal baseline.

In this patient, the authors found a significantly shorter LT and greater absolute and relative HR increase for seizures originating on the right hemisphere. They concluded that in view of a left-right difference in LT to ictal tachycardia onset of 6.3 s, which is shorter than the usual propagation delay of seizure activity between the two hemispheres, both hemispheres must influence the autonomic nervous system directly and independently from each other and not via a propagation to the right hemisphere, which has previously been suggested to be the dominant side in ictal autonomic regulation by Kato and colleagues (Kato et al., 2014).

We agree with the authors that their case is interesting and worthwhile being reported. However, single cases bear the risk of overinterpretation and invalid generalization, especially when considering physiological and biological features that tend to vary greatly between individuals. In fact, we have previously studied a group of 15 patients with TLE and independent seizure onset within both hippocampi as assessed by intracranial video-EEG monitoring using depths electrodes (Jordan et al., 2019, Surges et al., 2013). Our analysis revealed that in each patient the time course of HR and the extent of HR change during temporal lobe seizures arising from the hippocampus is very variable and does not depend on the side of seizure-onset on an *inter*-individual level. Nevertheless, in line with the case report in question, we observed an individually lateralized peri-ictal modulation of HR in some of our patients (Surges et al., 2013, Fig. 1A), challenging the "preceding tachycardia sign" as proposed by Kato and colleagues (Kato et al., 2014). Yanai and colleagues highlight the *intra*-individual lateralization of the LT and the relative and absolute HR

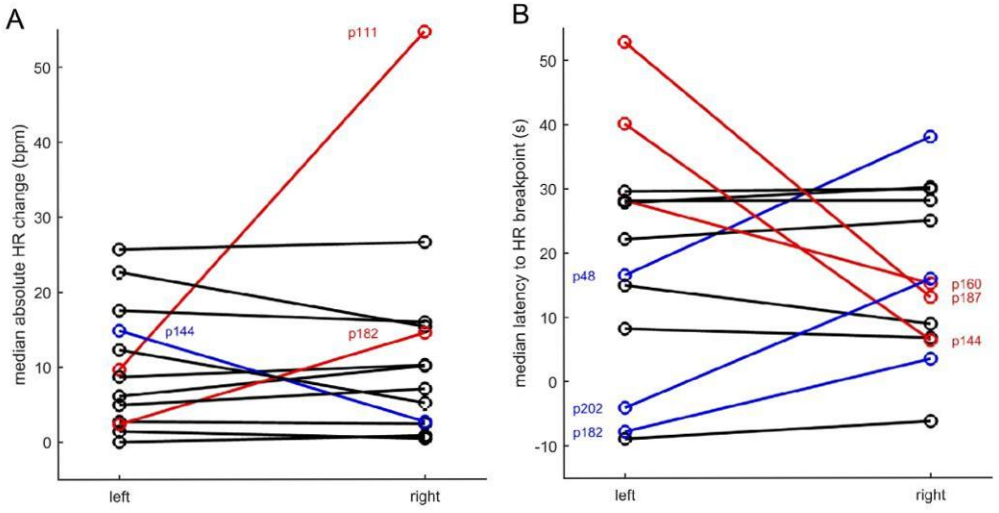

Fig. 1. Median absolute HR change as well as median latency to HR breakpoint is lateralized only in some patients with independent seizure onsets from both hemispheres. (A) Only 3 out of the 13 depicted patients (23%) show a difference in median absolute HR change of more than 10 bpm between left and right onset seizures (red for "right dominant" (n = 2), blue for "left dominant" (n = 1), black for no side difference (n = 9)). (B) Six out of 13 patients (46%) show a difference in median latency to HR breakpoint (Jordan et al., 2019) of less than 10 s when comparing right and left onset seizures (red for faster HR breakpoint onset on the right (n = 3), blue for faster onset on the left (n = 3), black for no side difference (n = 7)). Negative values indicate a HR breakpoint preceding the EEG seizure onset. Interestingly, not a single patient shows a lateralization for the same hemisphere in both parameters. Legend: graph labels = patient indices, each line representing one patient.

https://doi.org/10.1016/j.clinph.2020.08.019

changes with their case report, which makes it a valuable addition to the still ongoing debate of an asymmetrical representation of central autonomic networks. The latency to significant HR changes on an intra-individual level has not been published in our previous studies, but the results are provided in Fig. 1B. Only about half of the patients show a side difference in latency to the HR breakpoint of more than 10 s. Patients with earlier HR breakpoints following seizures from the left and right hippocampus are represented equally. A great advantage of our studies is the inclusion and analysis of patients with bilateral hippocampal depth electrodes, which allowed an accurate determination of the seizure onset. Subdural electrodes might not be as accurate in this respect since the seizure propagation from the temporo-mesial structures to the surface of the temporal lobe induces a certain time delay.

In summary, we agree with the authors' conclusions that both hemispheres play a role in the peri-ictal modulation of HR dynamics, but want to stress that this asymmetric modulation is individually lateralized in some patients, as previously reported (Surges et al., 2013; Jordan et al., 2019). These findings may be important for the recent efforts to develop automatic seizure detection devices based on heart rate and in the context of elevated cardiac risks in people with epilepsy (Shmuely et al., 2017).

Funding

No funding was received.

Author contributions

AJ drafted the first version, MB and RS revised the letter for important intellectual content.

Declaration of Competing Interest

The authors declare that they have no known competing financial interests or personal relationships that could have appeared to influence the work reported in this paper.

References

Jordan A, Bausch M, Surges R. Semi-automatic quantification of seizure-related effects on heart activity. Epilepsy Res 2019;157 106187.
Kato K, Jin K, Itabashi H, Iwasaki M, Kakisaka Y, Aoki M, et al. Earlier tachycardia onset in right than left mesial temporal lobe seizures. Neurology 2014;83 (15):1332–6.
Shmuely S, van der Lende M, Lamberts RJ, Sander JW, Thijs RD. The heart of epilepsy: current views and future concepts. Seizure 2017;44:176–83.
Surges R, Jordan A, Elger CE. Ictal modulation of cardiac repolarization, but not of heart rate, is lateralized in mesial temporal lobe epilepsy. PLoS One 2013;8(5) e64765.
Yanai K, Shimada S, Kunii N, Takasago M, Takabatake K, Saito N. Earlier tachycardia for seizures originating from the right versus left hemisphere in a patient with bilateral mesial temporal lobe epilepsy. Clin Neurophysiol 2020;131:2168–70.

Arthur Jordan *
Marcel Bausch
Rainer Surges
Department of Epileptology, University Hospital Bonn, Venusberg-Campus-1, D-53105 Bonn, Germany
* Corresponding author.
E-mail address: arthur_jordan05@web.de (A. Jordan)
Accepted 20 August 2020

Available online 17 September 2020

3. Danksagung

Allem voran danke ich meinem Doktorvater, Prof. Dr. Rainer Surges, nicht nur für die Einführung in die akademische und epileptologische Welt, sondern auch für das langjährige Mentoring in diversen Lebensfragen. Seine Tür steht für mich heute noch immer offen für angeregte und kreative Gespräche, in denen die Zeit erschreckend schnell verfliegt. Er verstand es immer, mich positiv zu verstärken und meine bisweilen umherschweifenden Ideen und Bemühungen in erstaunlich produktive Bahnen zu lenken. Wer hätte ganz zu Beginn gedacht, dass diese Dissertation den Grundstein für ein synergistisches Arbeitsverhältnis legen würde, in dem auch 12 Jahre später noch der kreative Enthusiasmus nicht aufhört zuzunehmen. Mein Dank gilt auch Dr. Marcel Bausch, mit dem mich nicht nur eine langjährige und sehr besondere Freundschaft, sondern auch die Passion für wissenschaftlich-technische Probleme verbindet. Seinem messerscharfen analytischen Verstand habe ich viele Fähigkeiten, die ich im Prozess der Erstellung dieser Arbeit erwerben konnte, maßgeblich mitzuverdanken. Nicht zuletzt danke ich meiner gesamten Familie, die mich über die Jahre stets mit Rückhalt und Motivation unterstützte.